ESC European Society of Cardiology

European Heart Journal - Imaging Methods and Practice (2025) **3**, qyaf043
https://doi.org/10.1093/ehjimp/qyaf043

SPECIAL ARTICLE

Patient centric performance and interpretation of SPECT and SPECT/CT myocardial perfusion imaging: a clinical consensus statement of the European Association of Cardiovascular Imaging of the ESC

Bryan Abadie [1,*], Riccardo Liga [2], Ronny Buechel[3], Andreas A. Giannopoulos[3], María Nazarena Pizzi [4,5,6,7], Albert Roque [5,6,8,9], Ricardo Geronazzo[10], Fabien Hyafil [11,12], Juhani Knuuti[13], Antti Saraste [13], Riemer Slart[14], Paul Cremer[15], Richard Weinberg[15], Maria João Vidigal Ferreira[16], Alessia Gimelli[17], and Wael Jaber [1]

[1]Heart, Vascular, and Thoracic Institute, Cleveland Clinic Foundation, Mail Code J1-5, 9500 Euclid Avenue, Cleveland, OH 44195, USA
[2]Cardiothoracic and Vascular Department, University Hospital of Pisa, Via Paradisa 2, 56100 Pisa, Italy
[3]Department of Nuclear Medicine, Cardiac Imaging, University and University Hospital of Zurich, Zurich, Switzerland
[4]Department of Cardiology, Hospital Universitari Vall d'Hebron, Passeig Vall d'Hebron 119-129, 08035 Barcelona, Spain
[5]Department of Nuclear Medicine, Nuclear Cardiology Unit, Hospital Universitari Vall d'Hebron, Passeig Vall d'Hebron 119-129, 08035 Barcelona, Spain
[6]Universitat Autònoma de Barcelona (UAB), Barcelona, Spain
[7]Centro de Investigación Biomédica en Red en Enfermedades Cardiovasculares (CIBER-CV), Madrid, Spain
[8]Department of Radiology, Hospital Universitari Vall d'Hebron, Passeig Vall d'Hebron 119-129, 08035 Barcelona, Spain
[9]Institut de Diagnòstic per la Imatge (IDI), Barcelona, Spain
[10]Cardioimaging at Diagnóstico Nuclear, Universidad de Buenos Aires, Av. Nazca 3449, C1417 CVE, Cdad. Autónoma de Buenos Aires, Argentina
[11]Nuclear Medicine Department, DMU IMAGINA, Hôpital Européen Georges-Pompidou, Assistance Publique - Hôpitaux de Paris, F-75015 Paris, France
[12]Université Paris-Cité, Inserm 970, PARCC, F-75015 Paris, France
[13]Heart Center, Turku University Hospital and University of Turku, Hämeentie 11, 20520 Turku, Finland
[14]Department of Nuclear Medicine & Molecular Imaging, University Medical Center Groningen, Hanzeplein 1, 9700 RB Groningen, The Netherlands
[15]Northwestern University, Suite 600 NMH/Arkes Family Pavilion, 676 N Saint Clair, Chicago, IL 60611, USA
[16]Faculty of Medicine, University of Coimbra, Coimbra, Portugal
[17]Fondazione CNR/Regione Toscana "Gabriele Monasterio", via Moruzzi n.1, 56124 Pisa, Italy

Received 26 March 2025; accepted after revision 28 March 2025; online publish-ahead-of-print 17 April 2025

Abstract

The non-invasive assessment of ischaemic heart disease with myocardial perfusion imaging remains an integral part of modern cardiology. This modality has been used for decades, but improving technology has maintained its relevance today. This document describes the fundamentals of single-photon emission computed tomography, including stress protocols, tracer pharmacodynamics, camera settings and capabilities, post-acquisition processing, and clinical translation in an easy to read and highly pictorial manner to be applicable to not only healthcare providers of all levels, but patients as well.

Keywords SPECT

* Corresponding author. E-mail: abadieb@ccf.org

Introduction

Non-invasive assessment of myocardial perfusion, function, and metabolic activity using radioactive tracers has been central in the care of patients with suspected or established coronary artery disease (CAD) for the past 50 years. Over that period, new tracers, cameras, computerized algorithms, and stress protocols have been introduced across the globe by different institutions and later adapted and endorsed by cardiovascular imaging professional societies [European Association of Cardiovascular Imaging of the European Society of Cardiology (ESC) and American Society of Nuclear Cardiology]. The performance of these tests requires an understanding of stress protocols, tracer pharmacodynamics and nuclear properties, camera settings and capabilities, post-acquisition processing, and finally, a comprehensive and clear reporting system to communicate with other health care providers. This final step is crucial in linking the technical aspects of the study to the clinical context.

This document sought to capitalize on the expertise and input of experts from both the USA and Europe. We will present a clear and concise document with numerous visual aids that will cover the performance of single-photon emission computed tomography (SPECT) cardiac imaging for patients with suspected or known CAD. The document and its figures/tables are meant to be utilized daily as a quick reference for the performance of these tests. In the spirit of patient centric care, this document can also be used through its visual cartoons to explain to individual patients their 'journey' on the day of a stress test. A hypothetical patient can follow specific charts of their tests to understand each step, tracer used, and time outside and under the camera. We aim to provide a comprehensive yet accessible document for testing facilities, trainees, established providers, and patients.

Stress protocols

Myocardial ischaemia occurs due to an imbalance between myocardial oxygen supply and demand. The goal of SPECT myocardial perfusion imaging (MPI) is to identify coronary plaques, who do not limit adequate myocardial blood flow at rest but interfere with the necessary increase in blood flow during exertion. The inability to provide the heart enough blood during exertion can result in angina, which typically manifests as chest, arm, abdominal, or jaw pain or shortness of breath. Obstructive coronary plaques can be identified in SPECT MPI via the differences in radiotracer uptake among the different segments of the myocardium. Areas of the heart downstream from obstructive plaque will take up less radiotracer than those without obstructive plaque during peak stress. Exercise and pharmacologic medications are the two most common ways to stress the heart and elicit heterogenous uptake of radiotracers.

Exercise works by increasing the heart rate and contractility of the heart, thereby increasing myocardial oxygen demand. Several exercise treadmill and exercise bike protocols exist for stress testing, such as the various Bruce, Cornell, and Naughton protocols. These protocols differ by speed, the rate at which the speed is increased, and the incline of the treadmill, with the Bruce protocol considered the most intense. No matter the protocol chosen, in an optimal exercise stress test, the patient will exercise for 8–12 min and achieve at least 85% of the max-predicted heart rate (220-age).[1]

Exercise protocols are preferred over pharmacologic protocols. They can more clearly link patient's symptoms to exertion, as well as provide additional prognostic data over pharmacologic stress testing. Exercise stress testing allows for the quantification of several metrics that have prognostic utility, such as the Duke Treadmill Score and the chronotropic response index.[2,3] While the functional capacity is predictive of mortality in each of the specific exercise protocols, the prognostic value is not transferable across different tests.[4] An additional advantage of exercise protocols is less artefact from gastrointestinal uptake due to greater shunting of blood flow away from the gastrointestinal tract.

When exercise is not feasible, a pharmacological stress test can be performed.[5] Pharmacologic stress testing typically uses either vasodilators (adenosine, dipyridamole, and regadenoson) or sympathomimetic agents (dobutamine) (*Figure 1*). The administration of nitrates prior to rest imaging can be performed to improve sensitivity in the assessment of viability in the setting of fixed perfusion defects.[6]

Vasodilators act via the adenosine receptor to cause coronary vasodilation; areas of myocardium distal to a flow-limiting stenosis will have impaired vasodilator response compared with normally perfused areas, creating a relative difference in tracer uptake. Common side effects from adenosine receptor agonists are flushing, dizziness, headache, shortness of breath, and chest pain.[7] Aminophylline, an adenosine receptor antagonist, can be administered to shorten the duration of adverse effects of adenosine receptor agonists.[5]

Dobutamine with or without atropine is the sympathomimetic agent of choice. Sympathomimetic drugs increase myocardial oxygen demand, and therefore can induce ischaemia, by increasing heart rate and contractility. Like exercise protocols, a patient undergoing dobutamine stress should aim to achieve 85% of max-predicted heart rate.[5] Patients who do not achieve adequate heart rate with dobutamine can be administered atropine.

Pharmacologic stress testing is preferred in patients who are unable to exercise, have an underlying left bundle branch block (LBBB) on electrocardiogram (ECG), are dependent on a ventricular pacemaker, or have uncontrolled atrial fibrillation.[8] Conduction disease can introduce artefacts that are less evident on vasodilator pharmacologic protocols.[9] (*Figure 2*). Data are emerging that the use of positron emission tomography/computed tomography (PET/CT) rather than SPECT with or without computed tomography (CT) may eliminate the 'artefactual' septal perfusion defects seen in patient with pacemakers or LBBB.[10]

In the case of a submaximal (non-diagnostic) exercise test when <85% max-predicted heart rate is achieved at peak effort, patients can in real-time be converted to a pharmacologic protocol. Pharmacological stress with a vasodilator can also be combined with low-level exercise to reduce side effects and improve image quality.[5]

Stress-ECG should be performed and reviewed by the interpreting physician with both exercise and pharmacologic stress protocols, as stress-ECG can show high-risk findings such as ischaemic ST changes, new conduction abnormalities, and atrial as well as ventricular arrhythmia.[11] Haemodynamic changes with exercise, such as a drop in blood pressure, can also be indicative of high-risk findings.

Patient preparation

Because patients who fail to reach adequate heart rate with exercise can be converted to vasodilators, all patients who present for SPECT MPI should be adequately prepped as if they will get a vasodilator.

Caffeine is an adenosine antagonist and can interfere with vasodilator stress testing. Caffeine-containing beverages, foods (chocolate, etc.), and caffeine-containing medicaments must be discontinued for at least 12 h prior to vasodilator stress.[6] Patients should exercise caution when consuming even decaffeinated beverages, as they may contain small amounts of caffeine that can interfere with the test. Methylxanthine containing medications, such as theophylline or aminophylline, must be withdrawn in vasodilator stress testing for at least five half-lives. Failure to adhere to proper preparation may require rescheduling the exam. *Figure 3* shows many examples of medications, food, and drink that may interfere with testing. Typically, patients are also instructed to fast and take nothing, except water by mouth for at least 4 h.[12]

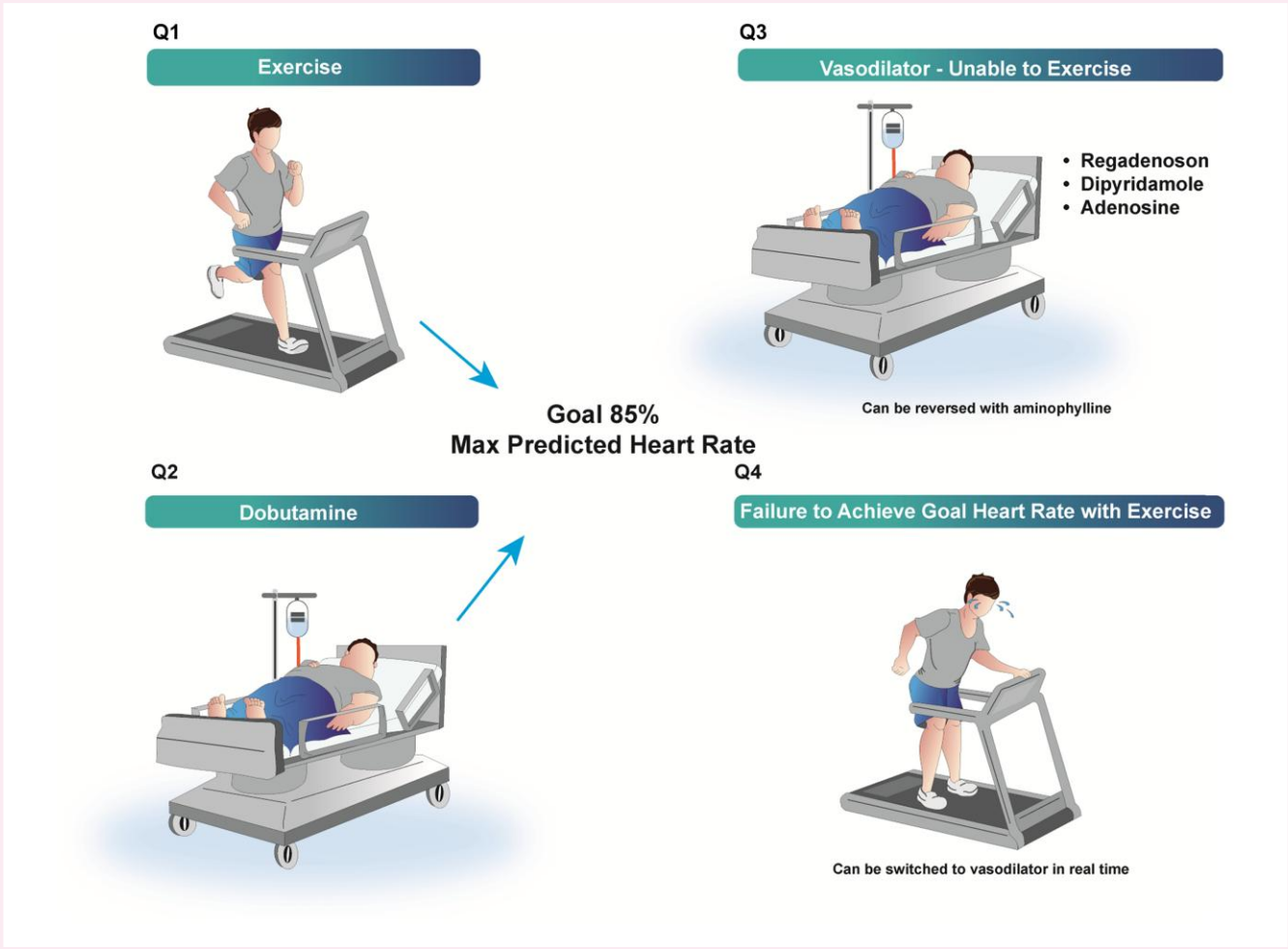

Figure 1 Exercise and pharmacologic stress protocols.

Before the test, the ordering clinician must decide on whether to interrupt haemodynamically active drugs, such as beta-blockers and vasodilators, based on the clinical indication for the test (e.g. diagnosis of ischaemia in naïve patients vs. assessment of the effects of anti-ischaemic therapy in patients with known CAD). If drugs are interrupted, the withdrawal should ideally last for three to five half-lives. Beta-blockers may interfere with achievement of adequate heart rate in exercise protocols leading to an increase in non-diagnostic studies. In vasodilator stress, beta-blockers may cause attenuation of perfusion heterogeneity, but only has a minor effect on quantitative MBF.[13–15]

More detailed information regarding patients' preparation, as well as general (contra)indications to cardiac stress tests have been covered in dedicated imaging guidelines, to which the reader is referred.[5,12]

Imaging protocols

The choice of imaging protocol and tracer dosage should be tailored to the patient and the specific clinical question by the referring physician within the wider context of an institution's capabilities and typical referral patterns. Each imaging protocol has strengths and weaknesses that must be balanced when choosing a patient centric, symptom driven, or risk stratification targeted stress test.[16]

^{99m}Technetium (^{99m}Tc)-sestamibi and ^{99m}Tc-tetrofosmin are the most commonly used perfusion agents. Unlike ^{201}Thallium, technetium tracers have no significant redistribution, and therefore separate injections are required to assess stress and resting perfusion.

The current protocols used for SPECT MPI are: (i) 1-day, low-dose stress, and high-dose rest; (ii) 1-day, low-dose rest, and high-dose stress; and (iii) 2-day protocol with equal radiotracer activity for stress and rest[12] (*Figures 4–6*).

The primary concern with 1-day imaging protocols is 'shine through', or residual activity from the first injection of tracer being counted when assessing the uptake from the second injection. In 1-day protocols, an adequate delay between rest/stress and stress/rest must be performed along with a higher radiation activity in the second injection. For instance, using ^{99m}technetium agents with a half-life of 6 h, after a 6 h delay, half of the tracer activity will remain and 'shine through' into the second set of images. Therefore, a two- to three-fold higher dose of injected activity is needed for the second injection to avoid a significant shine through effect.[12,17]

The other primary decision with 1-day imaging is whether to perform stress or rest imaging first. Stress-first protocols are preferred, as normal perfusion on stress imaging obviates the need for a rest injection, reducing radiation dose. However, stress-first protocols require real-time interpretation by clinicians that may not be easily incorporated into a clinical workflow. In some patients with a known previous infarction, it may be desirable to do the rest imaging first, allowing for

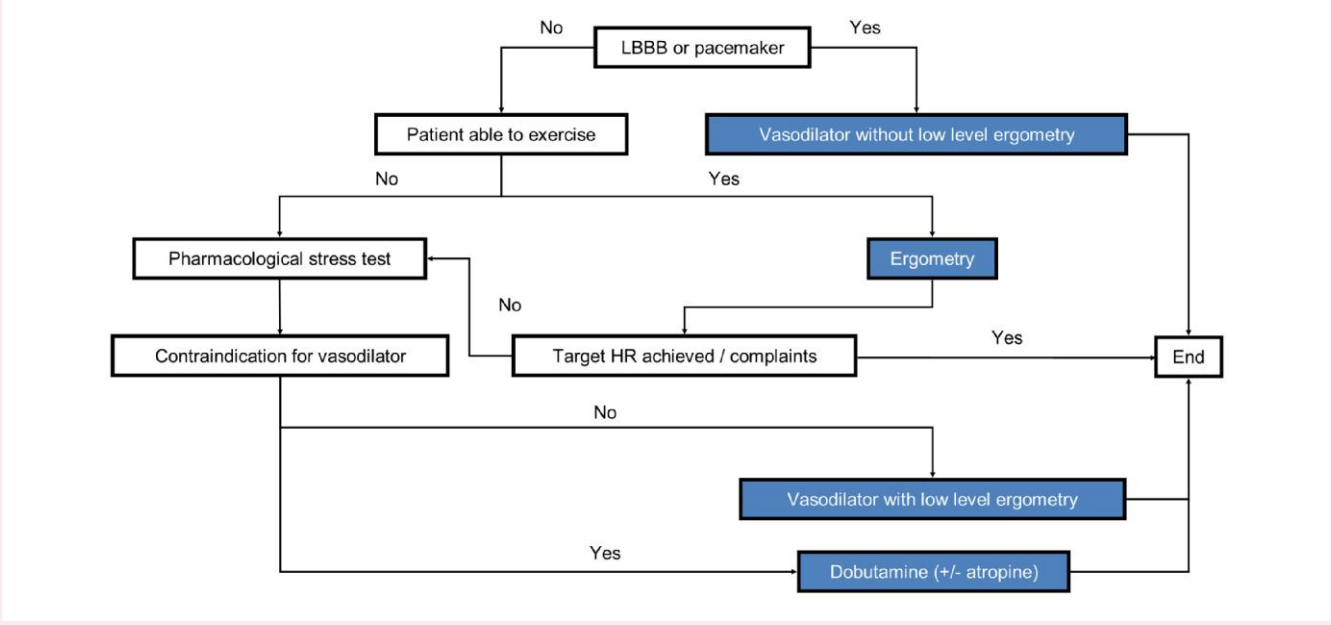

Figure 2 Flowchart to help decide best stress modality in the setting of conduction disease.

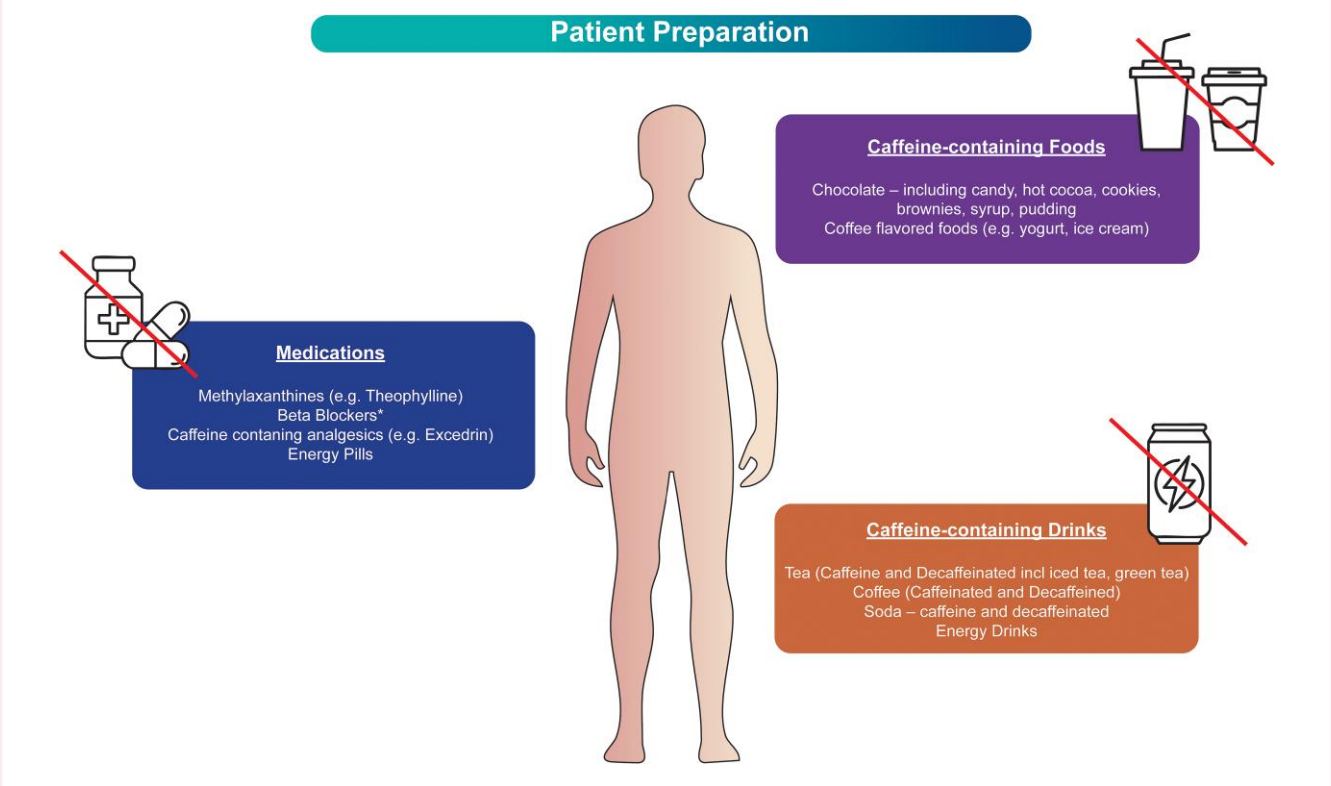

Figure 3 Patient preparation: examples of medications, caffeine-containing foods, and caffeine-containing drinks that can interfere study quality. *Some providers may wish to continue beta-blockers or vasodilators when the purpose of the exam is to evaluate the extent of ischaemia in the setting of medical treatment.

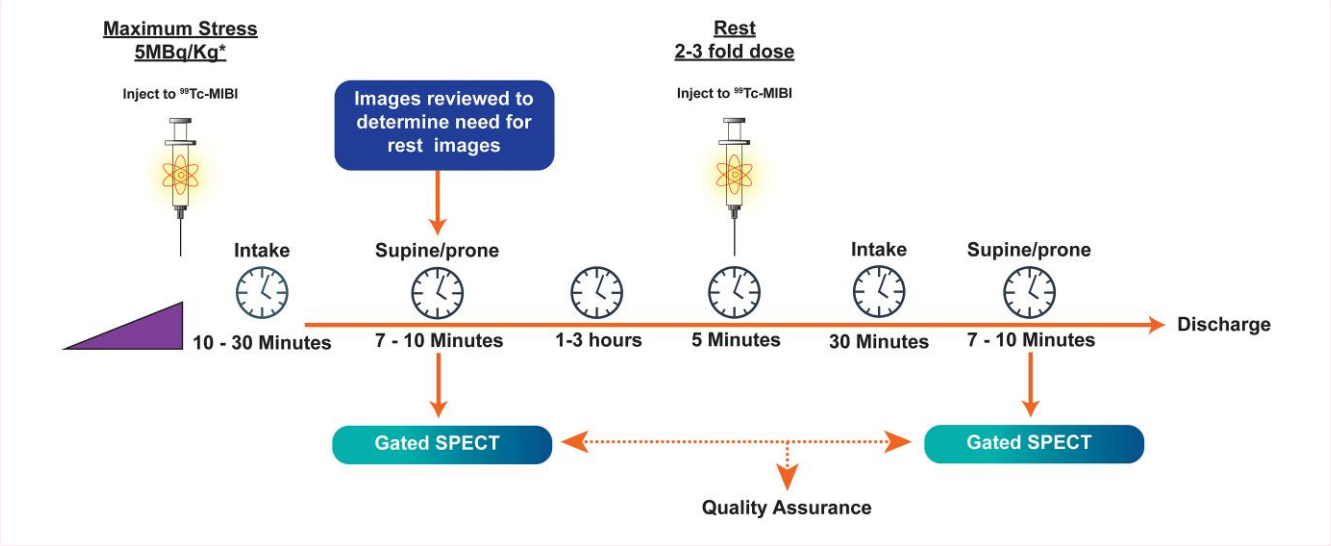

Figure 4 Standard 1-day stress/rest protocol. Note there is a two- to three-fold increase in dose with the second injection to avoid shine through, thus increasing the radiation exposure. Compared with 2-day protocols, 1-day protocols may be more convenient for patients. Prone imaging can be performed for attenuation correction in the absence of a hybrid SPECT/CT system. With hybrid systems, CT for attenuation correction or calcium scoring can be performed prior to the SPECT acquisition. *Note: tracer dose may differ based on type of SPECT system.

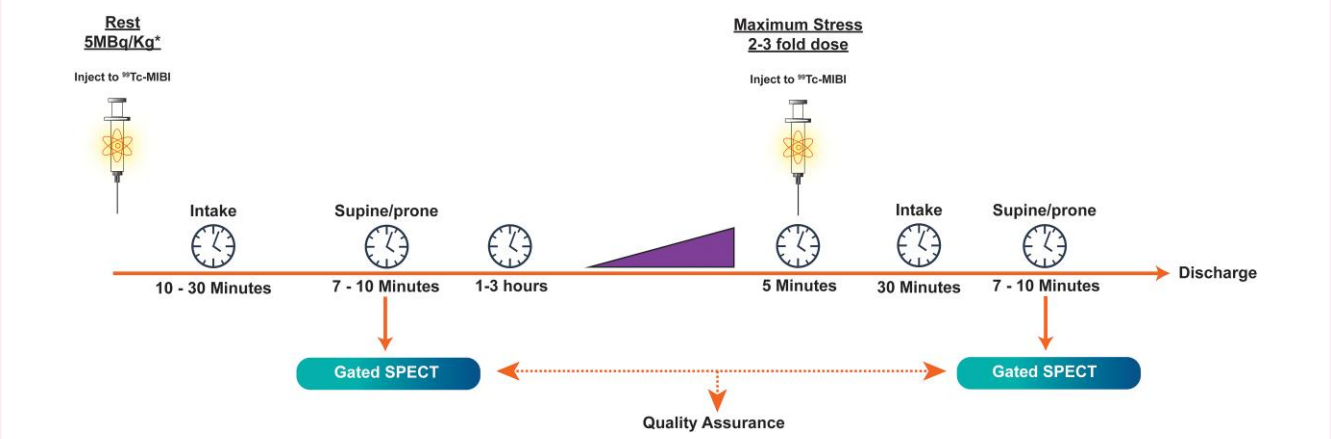

Figure 5 Standard 1-day rest/stress protocol. Note there is a two- to three-fold increase in dose with the second injection to avoid shine through, thus increasing the radiation exposure. Compared with 2-day protocols, 1-day protocols may be more convenient for patients. Prone imaging can be performed for attenuation correction in the absence of a hybrid SPECT/CT system. With hybrid systems, CT for attenuation correction or calcium scoring can be performed prior to the SPECT acquisition. *Note: tracer dose may differ based on type of SPECT system.

the addition of a viability assessment when appropriate. Additionally, performing rest images first also allows for the use of the higher dose of tracer, and therefore better image quality, for the stress images.

Alternatively, 2-day protocols use the same dose for the second injection, allowing for a further reduction in radiation exposure to patients and health care staff. Stress imaging should always be performed first, as normal stress imaging can similarly obviate the need for rest images in 2-day protocols. In patients with BMI $\geq$ 35 kg/m^2, a 2-day protocol is advised to avoid the very high ^{99m}Tc doses needed to obtain good quality imaging.[12,17] (*Figure 7*).

Gated imaging can assess left ventricular ejection fraction (LVEF) and left ventricular volumes. Acquisition can be performed earlier in treadmill and exercise bike protocols, typically between 5 and 10 min after stress injection. The earlier acquisition is more likely to detect a drop in the LVEF, an increase in volumes, and the index of transient dilation, which may indicate a high-risk exam. The ingestion of liquids can facilitate intestinal transit and eliminate excess subdiaphragmatic activity. Eating a high-fat meal before acquiring both post-stress and rest images may also remove artefact from the intestines. With pharmacological stress protocols, the advised post-stress acquisition time is 30–45 min

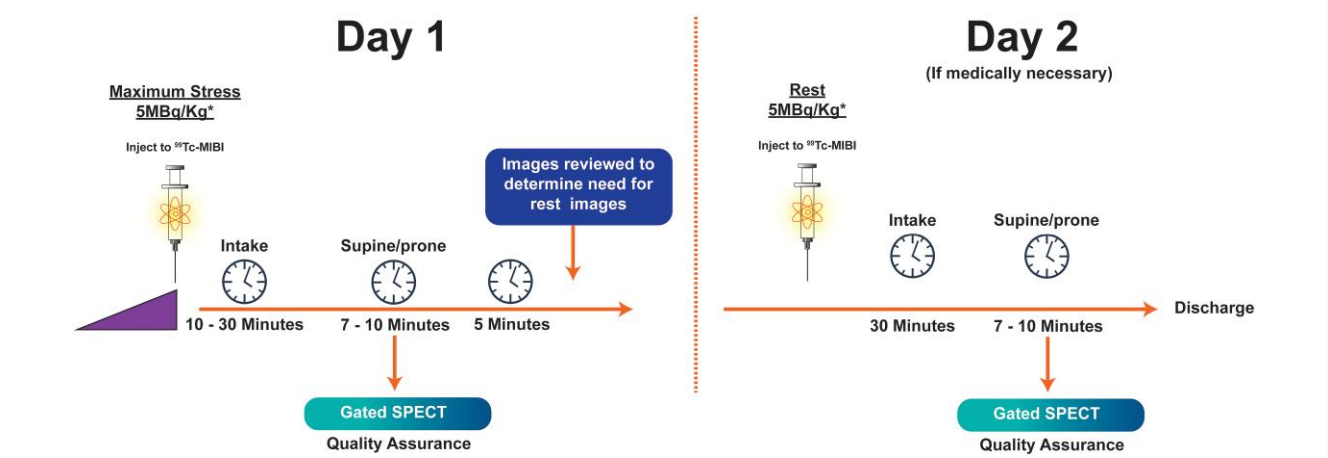

Figure 6 Standard 2-day protocol. Both rest and stress tracer injections are the same dose. Two-day testing limits radiation exposure but may be less convenient for patients, as it requires two trips to the imaging centre. Two-day protocols may be more logistically challenging as they require appointment times to remain open until a decision can be made about the need for rest imaging. Alternatively, 2-day protocols may decrease the number of hours a patient is in the imaging facility and may reduce camera downtime. Prone imaging can be performed for attenuation correction in the absence of a hybrid SPECT/CT system. With hybrid systems, CT for attenuation correction or calcium scoring can be performed prior to the SPECT acquisition. *Note: tracer dose may differ based on type of SPECT system.

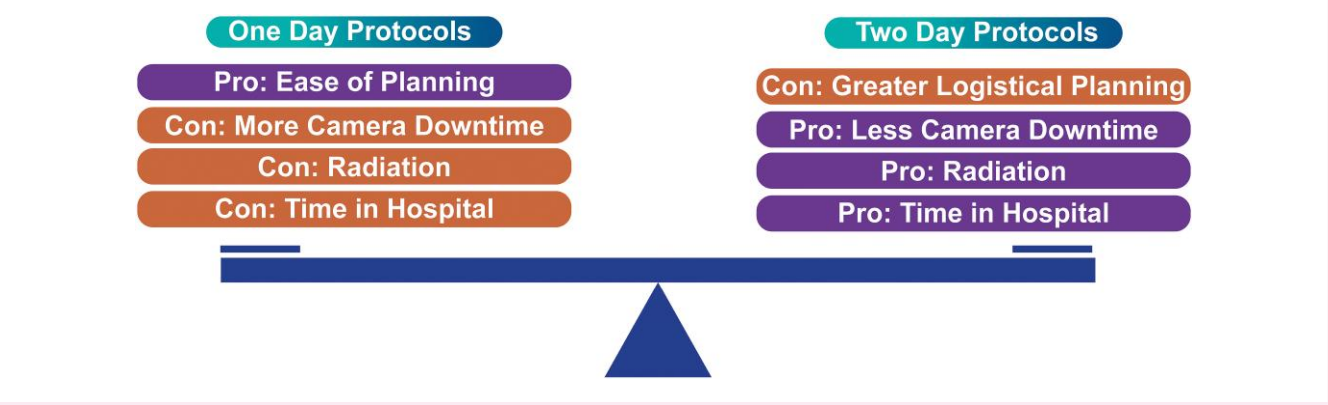

Figure 7 Two-day protocols have lower radiation dose, less time in the hospital, and less camera downtime compared with 1-day protocols. Depending on type of practice, 2-day protocols may present logistical challenges to coordinate.

to allow for lower GI activity and less likelihood of gut activity interference with cardiac activity and spillover effect.

Ultra-fast cameras with CZT detectors can substantially reduce the necessary tracer dose and acquisition times.[18,19]

Tracers

The ideal tracer for myocardial perfusion SPECT imaging should possess specific biochemical properties. It should be evenly distributed within the myocardium post-first-pass extraction from the blood and remain inert during imaging. It should emit high-energy gamma rays and have a short half-life. Finally, it should be cost-effective.

There are currently two commercially available radiopharmaceuticals for SPECT myocardial perfusion which are both ^{99m}technetium-based, Tc-sestamibi, and Tc-tetrofosmin. Both are produced in a generator and have a half-life of 6 h. 201-Thallium, a potassium analogue, should be avoided in contemporary clinical routine, given its suboptimal physical properties, low counts images, and—most importantly—relatively high radiation exposure.[5]

Camera specifications

In conventional nuclear cardiac imaging, the photons emitted by the radiotracers are detected and located by a scintillation device, also known as an Anger camera. Anger cameras have the following four main components[12] (*Figure 8*).

(1) *Collimator*: Parallel-hole collimation is the standard for cardiac SPECT imaging. This directional control is crucial for accurate imaging and reducing background noise. Collimators discard the greatest majority

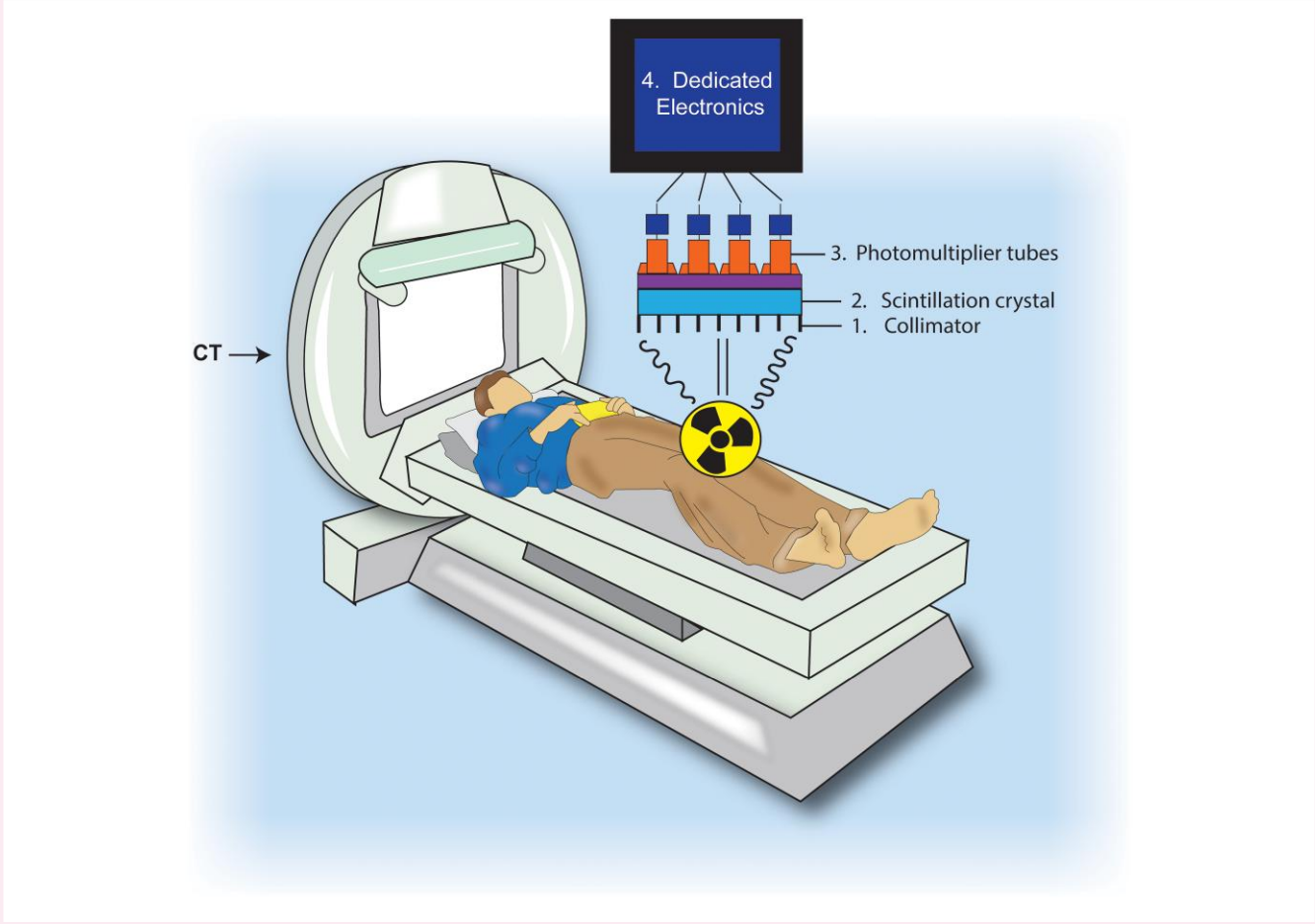

Figure 8 Typical gamma camera with collimator, scintillation crystals, photomultiplier tubes, and dedicated electronics.

(>95%) of the emitted photons and are the primary determinants of the spatial resolution of SPECT devices (i.e. 8–10 mm in range). The low-energy, high-resolution collimator is usually best for ^{99m}Tc.

(2) *Scintillation crystals*: Conventional cardiac SPECT cameras have sodium iodide (NaI) crystals that emit visible light when hit by high-energy photons and have an adequate sensitivity for detecting photons with an energy between 50 and 150 keV.

(3) *Photomultiplier tube*: The visible light produced by a scintillating crystal is converted into electronic signals and amplified by an order of 10^6 by the photomultiplier tubes. Photomultiplier tubes select only the photons that fall into the pre-specified energy spectrum of the employed radiotracer (i.e. energy window), defining the location of the scintillation event.

(4) *Dedicated electronics*: The electric pulses coming from the photomultiplier tubes are digitized by dedicated electronics that further amplify the incoming signals and create the digital pixels of the final image array.

Image acquisition

The most common cardiac SPECT systems consist of a dual-head device formed by two scintillation cameras positioned 90° apart. The two cameras generate 3D images by acquiring a series of static images over a 180° rotation centred on the left ventricular myocardium. As the camera rotates, multiple myocardial projections (usually 64) are acquired, each lasting 20–25 s, with a typical SPECT acquisition lasting ~15 min.[17]

The supine position is commonly used for conventional SPECT, with arms typically raised above the head, away from the field of view. A comfortable position should be confirmed with supports below the knees and arms and with appropriate belts. Importantly, arm position should be the same in both the rest and stress acquisitions to not introduce differing artefacts between the acquisitions. If available, supporting devices appropriate for gamma cameras can be used for the patient's comfort. Alternatively, prone positioning can be performed in men to avoid diaphragmatic attenuation. Supine and prone imaging can be used together to differentiate defects from attenuation artefact when other forms of attenuation correction are unavailable.[5,17]

Filtered back projection

During SPECT imaging, the rotation of the detector heads around the patient's chest leads to the overlapping of cardiac structures, such as parts of the apex projecting anterior to the base in certain views. Therefore, reconstruction algorithms are essential to correct for these issues.

Filtered back projection has been a popular method to reconstruct images since the 1970s. In back projection, the image projections are run back through the source to gain a greater approximation of the original image (*Figure 9*).

In filtered back projection, a high-pass filter is used to further eliminate blurring artefact. Consequently, filtered back projection generates images quickly with low computing requirements, but may impair specificity. Butterworth filters are also commonly used; these low-pass filters suppress high-frequency signals to improve image quality[21] (*Figure 10*).

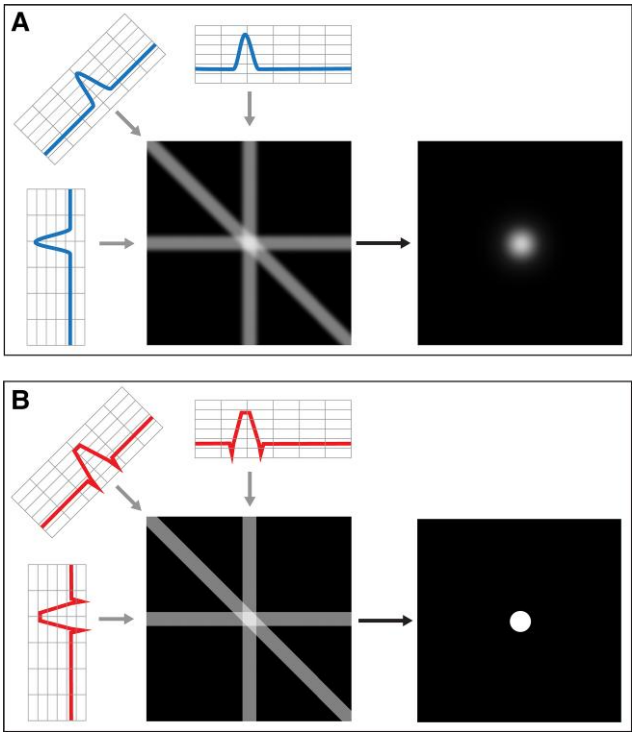

Figure 9 Unfiltered back projection (*A*) leads to smearing of the original view along the path it was originally acquired, resulting in a blurry image. During filtered back projection (*B*), each view is filtered before being back projected, resulting in an exact and sharp reconstruction of the original image. Reproduced with permission.[20]

Iterative reconstruction

Iterative reconstruction is the process of obtaining the best possible solution for an image by stepwise or successive approximation. A virtual, initial estimate of the activity distribution is made and compared with the actual acquired measurement. The virtual estimate is then updated, and the process is repeated a specified number of times, or iterations, until the change between the estimated and acquisition becomes minimal, having converged to the best possible solution.

Contrary to filtered back projection, no filtering is necessary to reach a solution through this process, but smoothing filters are commonly used to control for noise. The most refined algorithms are also able to further suppress noise while enhancing spatial resolution with a technique called resolution recovery[21] (*Figure 10*).

The primary limitation to iterative reconstruction had previously been its computational burden; with significant advances in computational power, iterative reconstruction has become much more feasible. The use of iterative reconstruction algorithms is strongly suggested to optimize signal-to-noise ratio, maintain spatial resolution, and reduce scan time and radiation dose.

Attenuation correction

Most photons emitted from the heart are deflected from their original linear path through the human body, leading to reduced count rates at the detector. Furthermore, such attenuation occurs heterogeneously due to the different densities of structures in the chest. SPECT, compared with PET/CT, is particularly susceptible to attenuation due to lower energy photons (*Figure 11*). Inadequately correcting for attenuation can impair specificity of SPECT.

Therefore, it is strongly advised to perform attenuation correction. Attenuation correction with CT is the preferred method to compensate for attenuation artefacts[22] (*Figure 12*). Alternatively, patient repositioning from supine to prone can offset some forms of attenuation artefact. More recently, machine-learning algorithms have been implemented to further compensate for attenuation.[9]

CT attenuation correction

Using maps of Hounsfield Units generated from CT, CT-based attenuation correction can be used to correct for common attenuation artefacts (e.g. breast or diaphragmatic attenuation). Evidence suggests that a single CT transmission scan can be used interchangeable for stress and rest imaging.[23]

In a hybrid SPECT–CT scanner, the SPECT detectors do not differ from a typical stand-alone SPECT system. The CT configuration can be low resolution, when exclusively for AC, or high resolution for dedicated coronary imaging. SPECT/CT systems typically have a large field of view (128 × 128 matrix with zoom factor of 1.0) and a variable-angle with dual detector systems for easy co-registration of SPECT and CT images.

Because all SPECT/CT studies are acquired sequentially, it is important that the patient be in the exact same position during and between each scan (apart from normal tidal breathing). Undesirable movement by the patient can cause a misregistration of the SPECT and CT images and artefactual perfusion defects (*Figure 13*).

Semiconductor cameras

Recently, cameras based on semiconductor detector technology, consisting of cadmium–zinc–telluride (CZT) crystals, have been

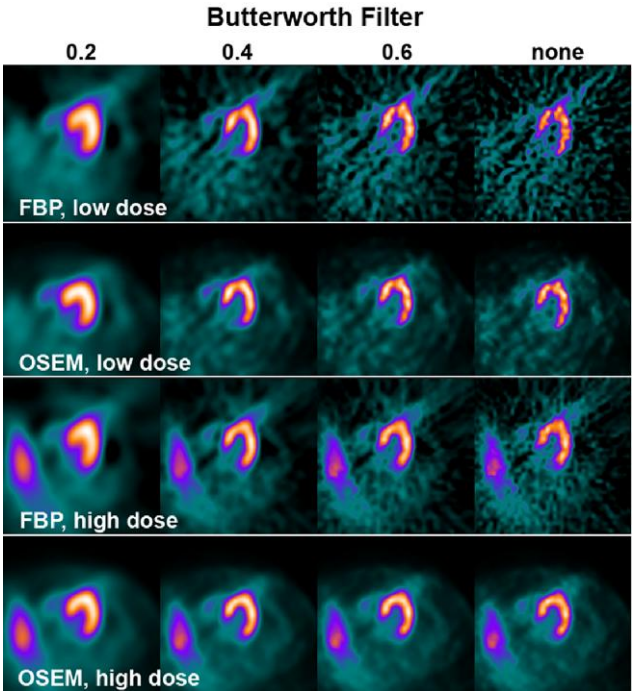

Figure 10 Filtered back projection (FBP) vs. ordered subset expectation–maximization (OSEM) iterative reconstruction for different total counts and with a butterworth post-processing filter at different intensities. *Low dose = 300 MBq 99mTc-tetrofosmin; high dose = 900 MBq 99mTc-tetrofosmin.* Reproduced with permission.[20]

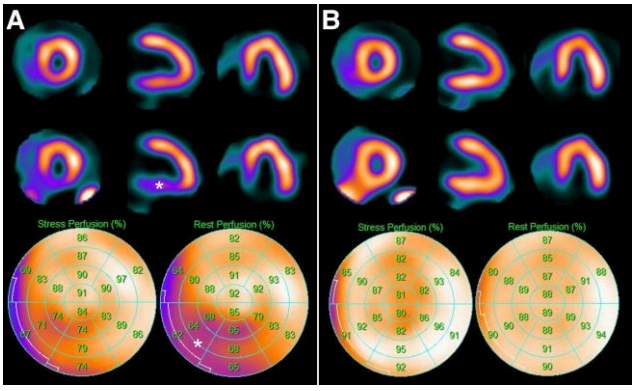

Figure 11 Myocardial perfusion SPECT imaging of a female patient with a body mass index of 29 kg/m^2. Selected slices (stress in the top row, rest in the bottom row) and corresponding polar plots of the reconstruction without attenuation correction (*A*) depict a reduction in counts particularly affecting the inferior wall. In contrast, attenuation corrected reconstructions (*B*) lead to a complete normalization, unmasking the apparent defect as an attenuation artefact.

developed.[17] These crystals directly convert photons into electrical pulses, eliminating the need for photomultiplier tubes. CZT crystals have smaller dimensions than NaI and, therefore, have a higher spatial resolution (4 mm). CZT detectors also have a linear count-rate response that can avoid the roll-off phenomenon at high count rates classically seen with photomultiplier tubes. As a result, CZT cameras have a 10-fold increase in system sensitivity and a 2-fold increase in image resolution compared with conventional SPECT cameras at the same injected dose. Consequently, tracer dose can be decreased while maintaining adequate sensitivity.[18,19]

In D-SPECT, a CZT-based system, there are nine individually rotating detector columns arranged on a stationary gantry in a curved configuration on the left side of the patient's chest. Each detector column comprises a CZT detector aligned with a square aperture from a parallel-hole collimator. Every detector column rotates at 110° independently of the other columns, allowing acquisition of hundreds of

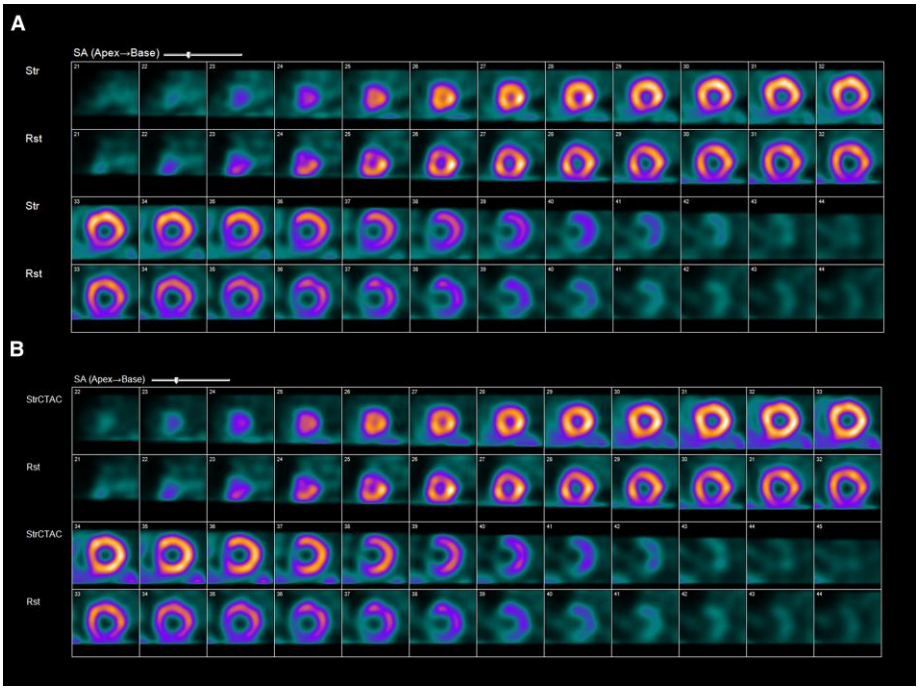

Figure 12 Panel (*A*) shows a fixed defect in the inferior wall. However, after CT attenuation correction, the fixed defect is shown to be artefact from diaphragmatic attenuation in Panel (*B*).

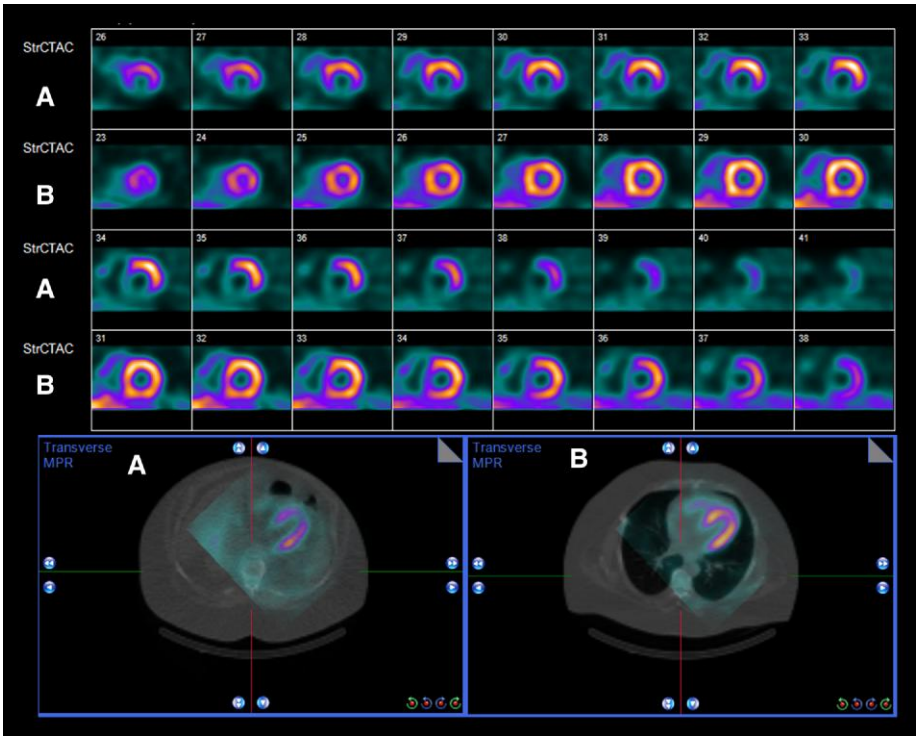

Figure 13 The initial images (*A*) suggest a large defect in the inferior wall. However, evaluation of the fusion images shows a misregistration artefact. When properly aligned (*B*), the perfusion is normal.

projections at varying angles of the heart. The tungsten collimators used with D-SPECT allow a higher percentage of photons to pass through compared with conventional low-energy, high-resolution collimators, yielding an eight-fold increase in acceptance of incidental photons. The reconstruction algorithms for D-SPECT are based on three-dimensional maximum-likelihood expectation–maximization iterative reconstruction. This algorithm helps overcome the loss in spatial resolution caused by the larger collimator holes.

D-SPECT alignment is myocardium-specific because of the smaller detectors and abridged field of view. Therefore, alignment requires a more precise centring of the heart compared with conventional systems. One risk with the smaller field of view of the D-SPECT is truncation artefact that can occur if the heart is not within the field of view of the scanner. Although rarely a problem, patients with severe cardiomegaly may pose issues to the imaging technologist if the heart is larger than the field of view. Drawing accurate left ventricular regions of interest from the initial pre-scan assessment and at processing of the images is necessary for proper quality control.

An additional advantage of D-SPECT is the ability to obtain dynamic acquisition and therefore quantify myocardial blood flow, a capability unavailable to conventional SPECT systems due to geometric and sensitivity limitations.

Another unique aspect of the D-SPECT system is that patients are imaged while sitting and can be positioned upright or supine. A limitation of D-SPECT compared with conventional SPECT/CT systems is the absence of CT imaging for attenuation correction and therefore the inability to assess for coronary calcification (*Figure 14*).[24]

Image display and interpretation

Images should be displayed and interpreted using dedicated workstations and software. Rotating raw projection images should be reviewed

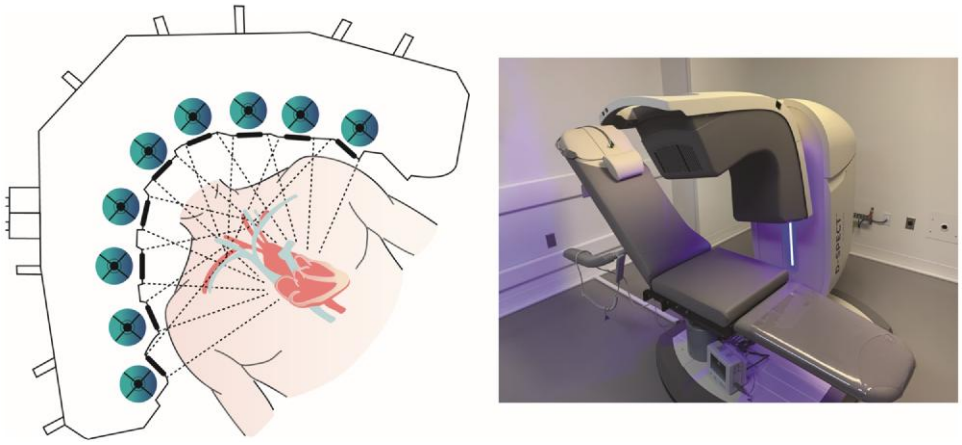

Figure 14 The D-SPECT is a CZT-system with nine rotating detector columns arranged over a stationary gantry (left). CZT-based cameras have the capability to reduce radiation dose and shorten imaging time. The D-SPECT system can also improve comfort by imaging patients while sitting (right).

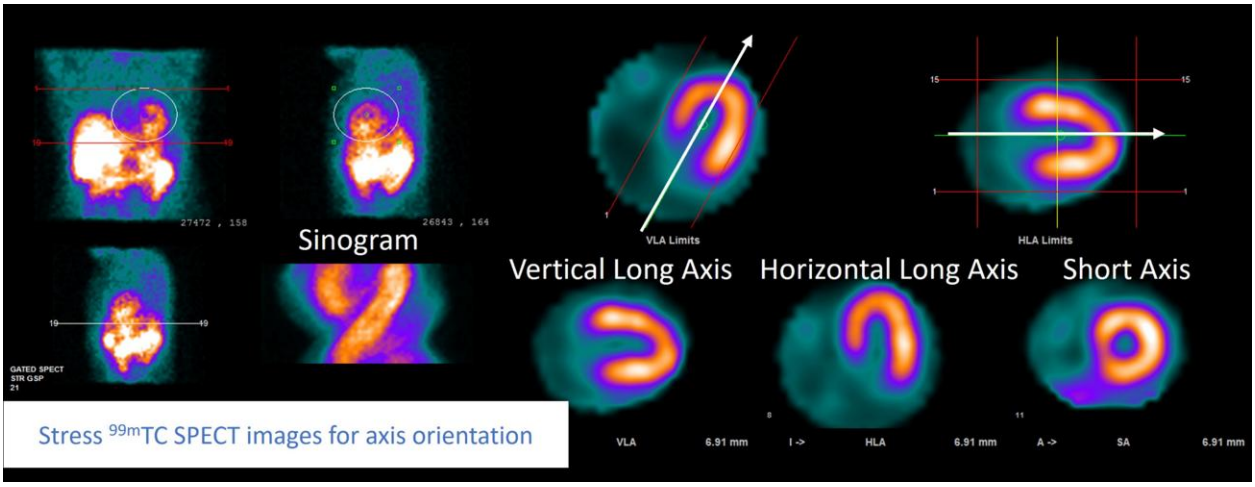

Figure 15 Shows the quality review panel with the orthogonal projection views of the raw-data (left) with an elliptical region of interest circumscribing the heart. This figure also displays the sinogram and the transaxial images for axis orientation and ventricular limits determination.

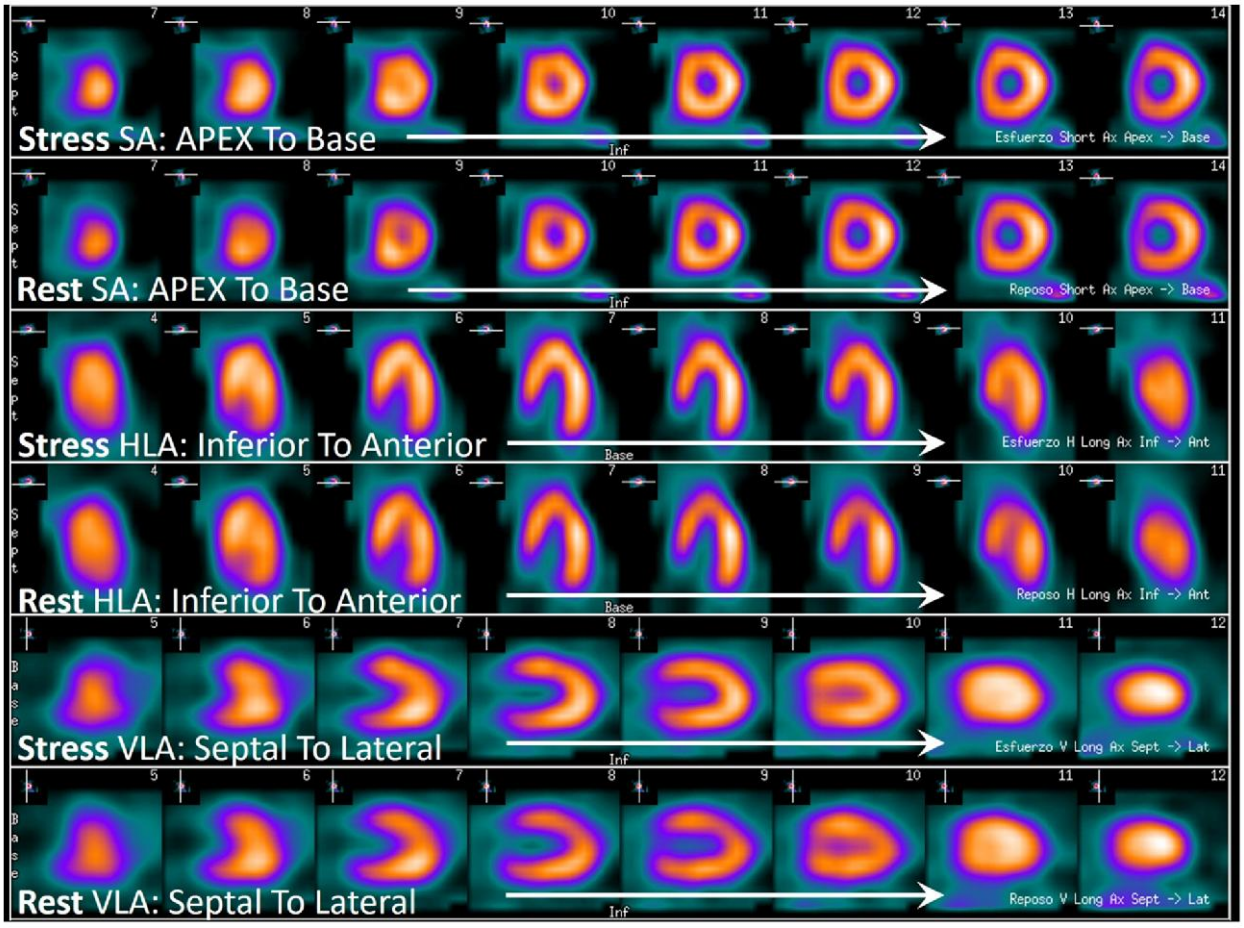

Figure 16 Shows the standard review panel of the spread-out tomographic slices of the left ventricle, conventionally the stress images are located above the rest images in the three axes. SA, short axis that runs from apex (left) to base of de ventricle (right); HLA, horizontal long axis that runs from inferior (left) to anterior wall of de ventricle (right); VLA, vertical long axis that runs from septal (left) to lateral wall of de ventricle (right).

in cine mode to check for the patient's movements and identify any extracardiac activity. The standard tomographic representation of the left ventricle is short axis (SA), vertical long axis (VLA), and horizontal long axis (HLA). Traditionally, stress imaging is displayed on top and rest imaging below (*Figures 15* and *16*).

Polar maps, colloquially known as bull's eyes, show the tracer uptake in a compact, two-dimensional representation of a three-dimensional left ventricle. Polar maps can be used to standardize perfusion, end of systole and diastole perfusion, and wall motion and thickening. Polar maps are useful for visualizing and quantifying percent of ventricular involvement. There is a standardized nomenclature for each segment[25] (*Figures 17* and *18*).

Perfusion defects are classified as fixed defects, which remain unchanged in both stress and rest perfusion, and reversible defects, that are present on stress, but not rest imaging. Fixed and reversible defects can co-exist within a single vascular territory. Reversible defects typically represent ischaemia. Fixed defects, reversible defects, or a combination of both can be seen with chronic total occlusions. SPECT can be used for viability assessments, although positron emission tomography is the preferred modality, when available.

The severity of a perfusion defect in each of the 17-segments on the stress and rest images is scored semi-quantitatively using a 0–4 score, with 0 being normal (*Figure 19*). The sum of each segment on stress imaging is termed the summed stress score (SSS); the sum on rest imaging is termed the summed rest score (SRS). Subtracting the SRS from the SSS yields the summed difference score (SDS), which represents the total ischaemic burden.

When reporting perfusion defects, clinicians should report both the size and severity of the defect. A defect can be small (1–2 segments), medium (3–4 segments), or large (≥5 segments). The severity of a defect, based on summed scores, can be normal or equivocal (≤3), mild (4–8), moderate (9–12), and severe (>12)[25] (*Table 1*). The SSS can also be used to determine the percent of myocardial involvement, an additional method of reporting the risk of an exam.[26] The percent myocardium abnormal, whether ischaemic or scarred, is calculated as sum of perfusion defect/68.[25]

Because SPECT MPI relies on relative differences in perfusion between the coronary arteries, it may miss balanced ischaemia in the setting of 3-vessel disease. Several high-risk findings have been described to aid in identifying this phenomenon, including transient ischaemic dilatation (increase in left ventricular size post-stress), a drop in LVEF with stress, and an increase in lung-to-heart tracer ratio.[27–29]

ECG-gated acquisition of counts allows quantification of LVEF and systolic and diastolic volumes (*Table 2*). Gated myocardial perfusion images can use either 8 or 16 frames per systolic cycle (*Figure 12*). The quality of gated left ventricular assessment will depend on the dose administered, the acquisition time, and the sensitivity of the

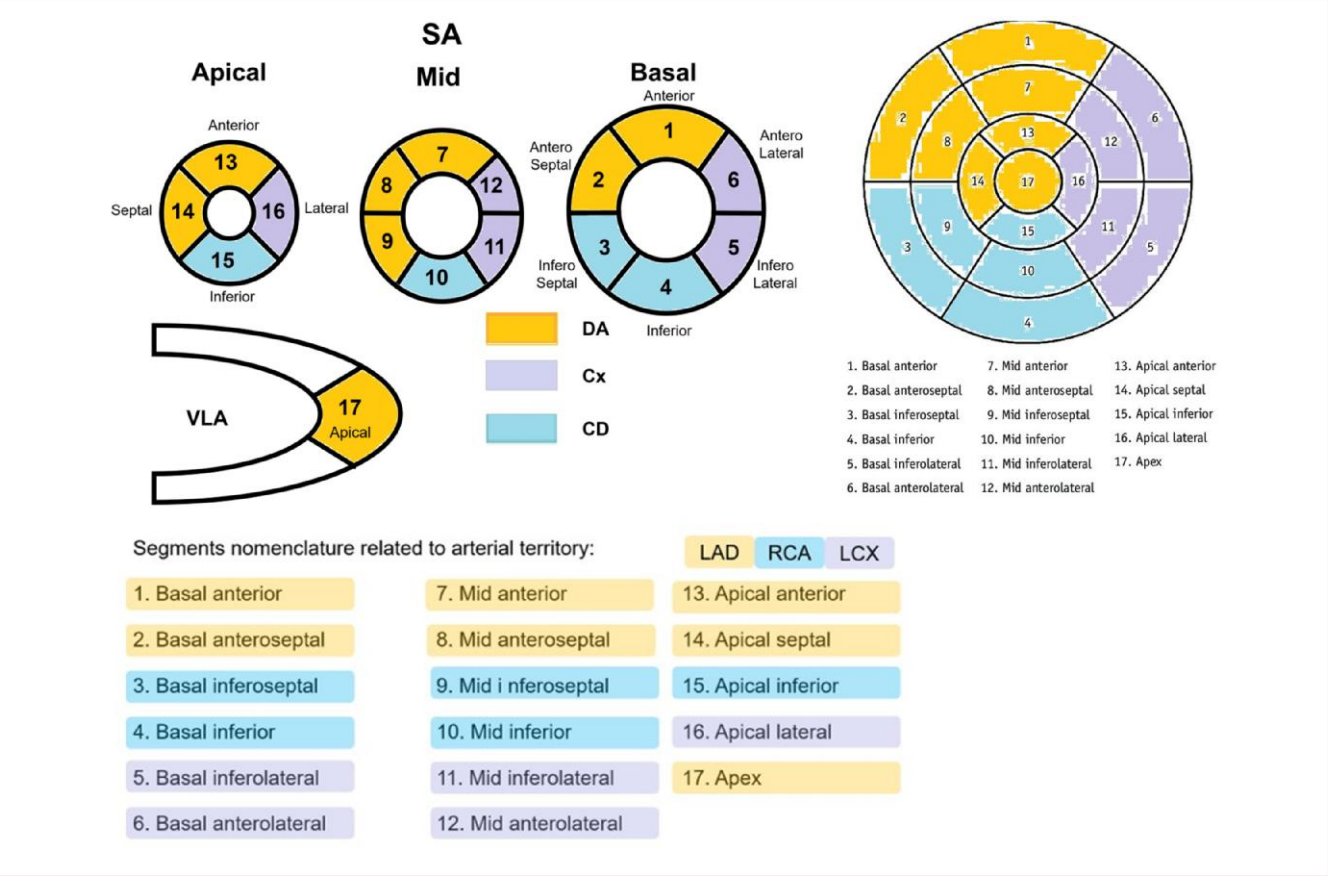

Figure 17 Shows the standard segmentation used to name the 17 segments of the left ventricle, extrapolated to the right on a generic polar map, in turn correlating each arterial territory. LAD, left anterior descending artery; RCA, right coronary artery; LCX, circumflex artery.

detectors. Both stress and rest LVEF and volumes should be reported, as a significant drop in LVEF or a significant increase in volumes from rest to stress could signify high-risk CAD. Whereas LVEF and left ventricular volumes by SPECT correlate well with magnetic resonance imaging, the gold-standard for these measurements, there can be significant deviations on a patient to patient basis.[30] Clinicians should therefore exercise caution with SPECT-derived left ventricular function, particularly in patients with small chamber sizes.

Wall motion on gated MPI should be reported in the standard 17-segment polar map. When evaluating wall motion, the software should allow the user to scroll through any of the slices in cine mode. Each view should be normalized to the series of end-diastolic to end-systolic slices to maintain the count density changes during the cardiac cycle that reflect myocardial wall thickening[25] (*Figures 20* and *21*).

Wall motion is important to report as it can help differentiate scar from areas with artefact from attenuation, improving the specificity of SPECT MPI. Scarred segments have reduced or absent wall-thickening compared with attenuated segments where wall-thickening should be normal[25].

Common reasons for artefacts and non-diagnostic studies

Artefacts

Artefacts are common in SPECT imaging, impairing diagnostic confidence[9] (Table 3 and *Figures 22–25*).

Inadequate vasodilator response

False-negative scans can occur when patients undergoing vasodilator MPI do not have an adequate response to the vasodilating medication. This can occur either due to exposure to caffeine or methylxanthines or due to extravenous infiltration of the vasodilator. Traditionally, haemodynamic parameters have been used to assess vasodilator response (e.g. drop in systolic blood pressure and increase in heart rate); however, these findings are not always reliable. A decrease in radiotracer uptake in the spleen during stress compared with rest, termed splenic switch off, can be assessed both qualitatively and quantitatively to determine vasodilator response.[36] A potential weakness of the smaller field of view with CZT SPECT is inadequate visualization of the spleen.

Radiation dose

The potential adverse effects of ionizing radiation, which can be divided into stochastic and deterministic types, are a primary concern in MPI.[37] Deterministic effects are clearly defined and have specific thresholds, whereas stochastic effects, such as the potential for cancer development decades later, are unpredictable and challenging to evaluate.[31] This risk estimation for stochastic effects stems largely from extrapolations of data from atomic bomb survivors to the ranges of radiation encountered in medical imaging. Despite the low levels of radiation associated with MPI, the cumulative radiation dose has doubled over the last 40 years, largely due to an increase in medical imaging.[32,38] *Table 4* summarizes the commonly applied effective doses for different

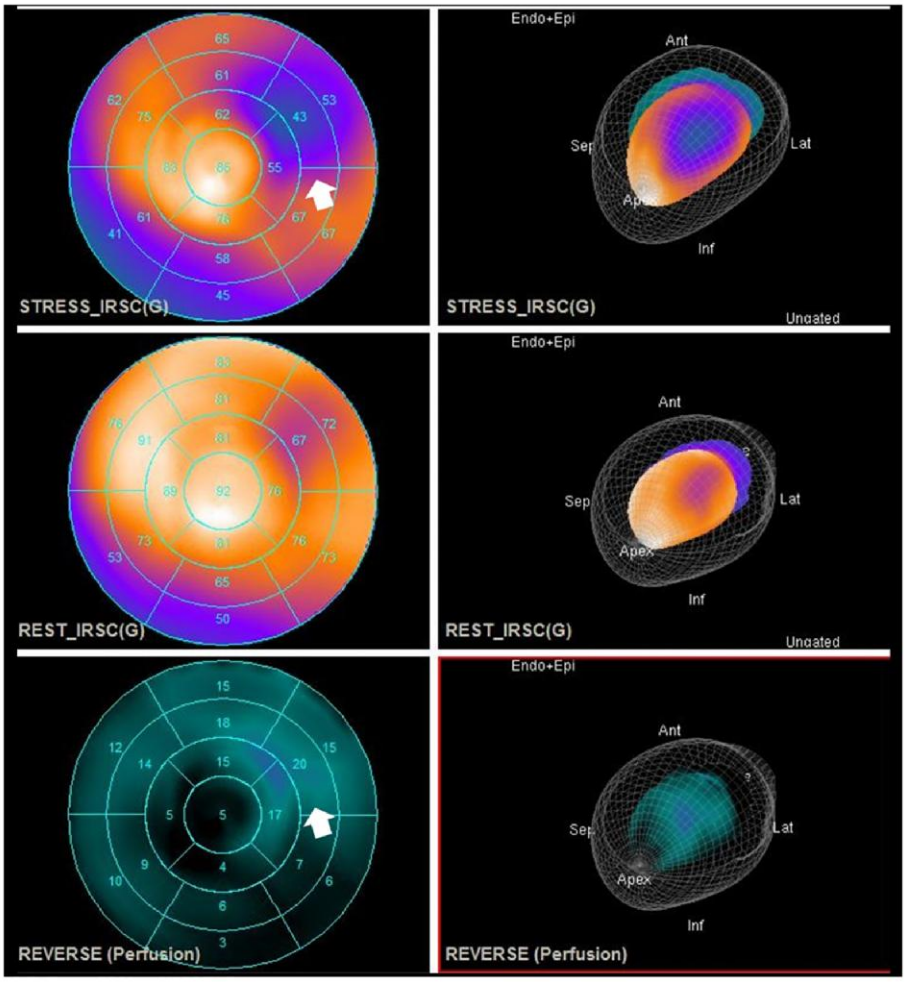

Figure 18 Polar maps showing a perfusion defect at peak stress in the circumflex artery territory which reverses at rest. Ischaemia (reversibility of the defect) is shown in the lower map. On the right you can see the correlation in the 3D rendering of the myocardium adjusted to perfusion.

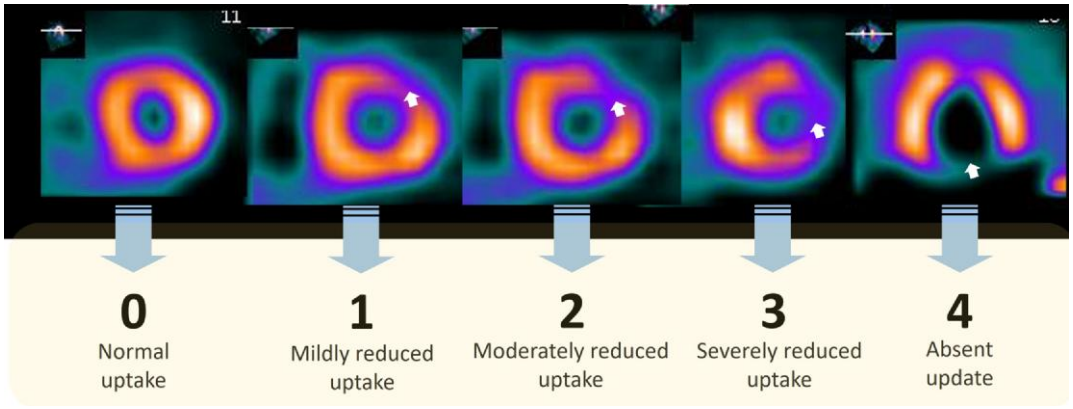

Figure 19 Shows the level of myocardial involvement (arrows) according to the visual hypoperfusion score, where 0 corresponds to normal perfusion, 1 is equivocal, 2 is moderate, 3 is severe hypoperfusion, and 4 is absent.

protocols and technetium tracers. *Figure 26* displays a comparison of radiation exposure for common cardiac imaging modalities.

Although radiation exposure in nuclear MPI is inherent to the nature of the procedures, considerable efforts have been made in the past decade to minimize radiation exposure without compromising diagnostic quality (*Figure 27*).[39]

First and foremost, adherence to appropriate use criteria can ensure MPI is reserved for clinically indicated cases.[31] Hardware (scanners) as well as software (i.e. image reconstruction) innovations now enable low-dose imaging that maintains high-image quality. For SPECT imaging, the use of novel technology, such iterative image reconstruction or CZT-based camera systems, has directly contributed to a significant reduction in effective radiation dose.[33]

Table 1 The criteria to quantify myocardial compromise according to the score obtained in the sum of the compromised segments

Summed score	≤3	Normal or equivocal
	4–8	Mild defect
	9–12	Moderate defect
	>12	Severe defect

Table 2 Categorization of ventricular function by left ventricular ejection fraction

Normal	55–70%
Low normal	50–55%
Mildly	45–50%
Moderately	35–45%
Severely reduced	≤35%
Hyperdynamic	≥70%

Computed tomography for SPECT/CT, including incidental findings

Attenuation correction with CT is advised to improve the diagnostic accuracy of SPECT MPI.[40–42] The CT scan is obtained either pre- and/or post- the radiotracer emission scan, and the patient must remain still to avoid misregistration artefacts. The field of view for the CT scan should include the chest to avoid truncation artefacts in the attenuation corrected images.

Importantly, the protocol of the CT performed for attenuation correction is not optimized for diagnostic chest or cardiac imaging. The tube current is typically much lower (e.g. 20 mAs) than a coronary calcium scan or coronary CT angiogram, and the slice thickness is also larger (e.g. 3–5 mm). In addition, no intravenous contrast is administered, ECG gating is not performed, and deep inspiratory breath holds are avoided.

Nonetheless, important clinically actionable findings may be present and should be reported.[43] In general, the most common findings are related to cardiovascular (*Figure 28*) or lung abnormalities (*Figure 29*). Distinct coronary calcifications should be noted and can be reported as binary (present or absent) or according to categories (mild, moderate, or severe). Aortic valve leaflet and mitral annular calcifications should be noted as these findings may be indicative of underlying valvular heart disease. Dilation of the ascending thoracic aorta (i.e. >4.0 cm) or pericardial effusions may also prompt further dedicated evaluations. Regarding lung findings, any pulmonary mass, infiltrate, or pleural effusion should be noted. Small lung nodules are often not well delineated and are overwhelmingly benign, though larger nodules (≥6 mm) may be evident. When available, prior dedicated chest or cardiac CT imaging and reports should be reviewed.

In certain patients without known coronary atherosclerosis, a dedicated coronary artery calcium scan can be included as part of the cardiac SPECT examination (*Figure 30*). If included, the patient should not have an elevated heart rate (i.e. >75 beats per minute) because images are obtained with a prospectively ECG-triggered axial acquisition at 65–80% of the cardiac cycle. Given this mid-diastolic and inspiratory breath-hold acquisition, the coronary artery calcium scan cannot be used for attenuation correction. In patients without known CAD, the coronary artery calcium score provides additional diagnostic and prognostic value. Specifically, patients with a coronary artery calcium score of 0 are less likely to have flow-limiting CAD; the calcium score also

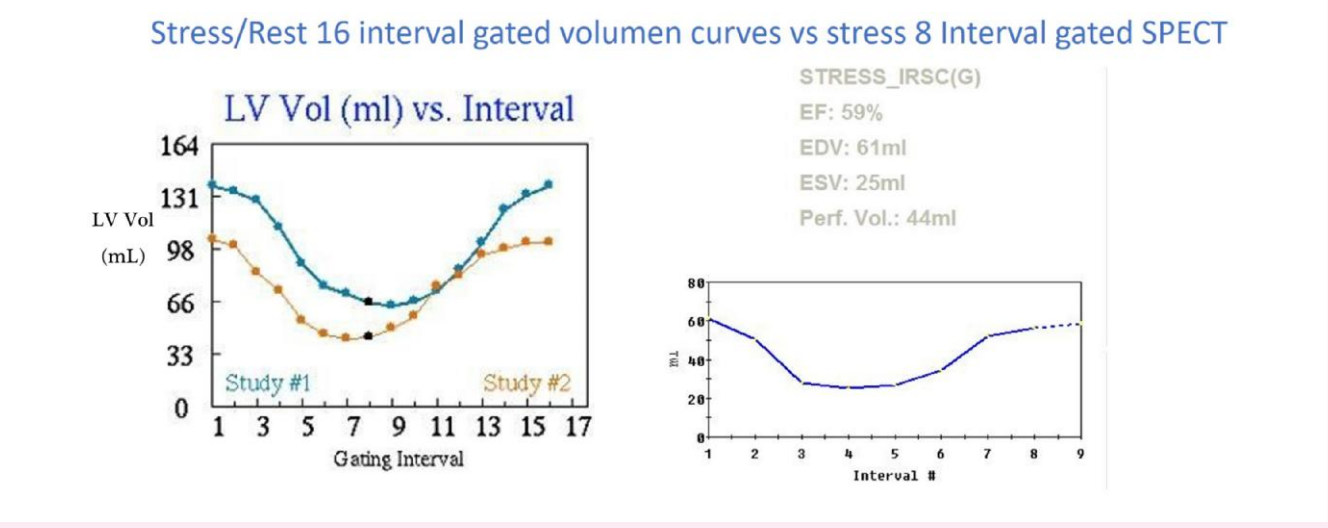

Figure 20 Two different types of acquisitions of gated imaging for quantification of ejection fraction and volumes are shown: on the left, volume curves acquired with 16 intervals between R-R of the ECG and on the right with 8, reconstructed with different commercial software.

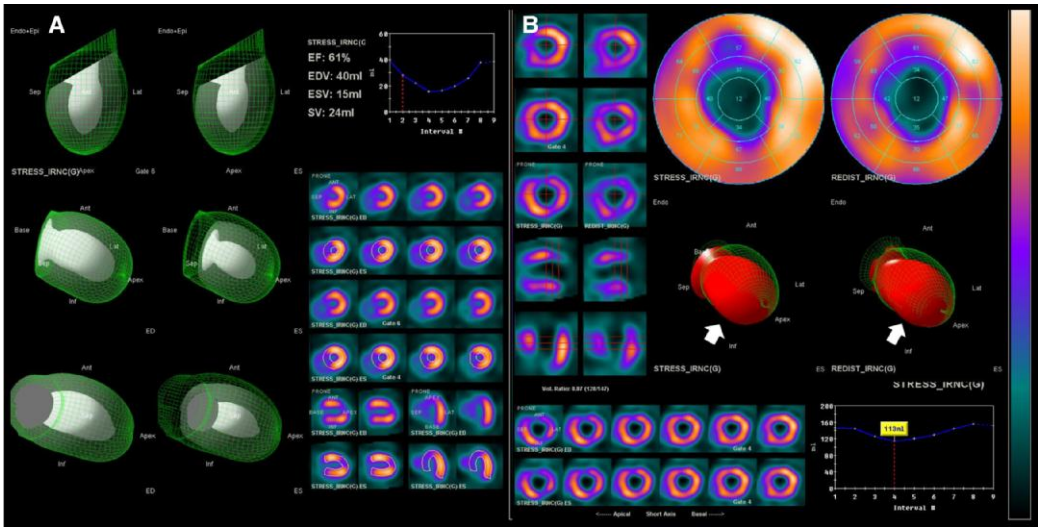

Figure 21 Panel (*A*) shows a gated SPECT with normal function and motility, with preserved thickening in a hypertrophic left ventricle. Panel (*B*) shows a patient with an anterior myocardial infarction and an anterior and septal dyskinesia (arrows) with severely depressed ejection fraction.

Table 3 Features associated with artefact generation and potential interventions to remedy artefacts

	Causes	Consequence	Intervention
Patient related	Movement: • Involuntary • Pathological • Accidental movement	• False perfusion defect or hiding a real perfusion defect (*Figure 15*)	• Revise motion correction • Check Cine Raw tomographic data • Re-image patient
	Body habitus	Attenuation defects (*Figure 14*)	• Supine/Prone imaging • CT attenuation Correction
	• Poor trigger signal • Cardiac arrhythmias	Poor quality images, sinogram showing missing data	• Reacquire • Adjust window frame/bin length on 90–100%
	• Left bundle branch block • Lateral hypertrophy	Hypoperfused septum	• ECG analysis clinical history
	• Septal hypertrophy	Hypoperfused lateral wall (*Figure 17*)	• ECG analysis clinical history
Positioning	• Miss centred silhouette • Arms position	Truncation of the heart	• Reacquire centred images
Tracer distribution	Extracardiac	Abnormal areas of focal increased or decreased uptake can lead to perfusion artefacts Excessive uptake: • Gall bladder • Liver • Bowel	• Mask projections and slices • Check radiotracer labelling efficiency • Iterative reconstruction methods
Tracer activity	Low count statistics • Low-dose injection (weight/dose mismatch) • Injection site in field of view • Extravasation	• Blurry images and poor quality gated • Low myocardial uptake	• Set acquisitions with extra time • Reacquire • Reinject in case of extravasation • Check radiotracer labelling efficiency

Continued

Table 3 ***Continued***

	Causes	Consequence	Intervention
Processing and Reconstruction	Orientation • Inappropriate axis plane selection • Misregistration on SPECT–CT	False perfusion defects	Reorientation
	Polar Map display • Inappropriate valvular plane selection in non-gated slices	• Enlarge or diminish true defects • Alter TID values (*Figure 16*)	Verify valvular plane (LV base limit)
	Gated SPECT • Misdetection of end systole/ diastole limits slices in gated frames	Under or overestimation of LVEF and volumes	• Analize volumes LV curves to ensure adequate calculation of LVEF and chamber volumes • Readjust acquisition to 8 or 16 frames

TID, transient ischaemic dilatation; LVEF, left ventricular ejection fraction.

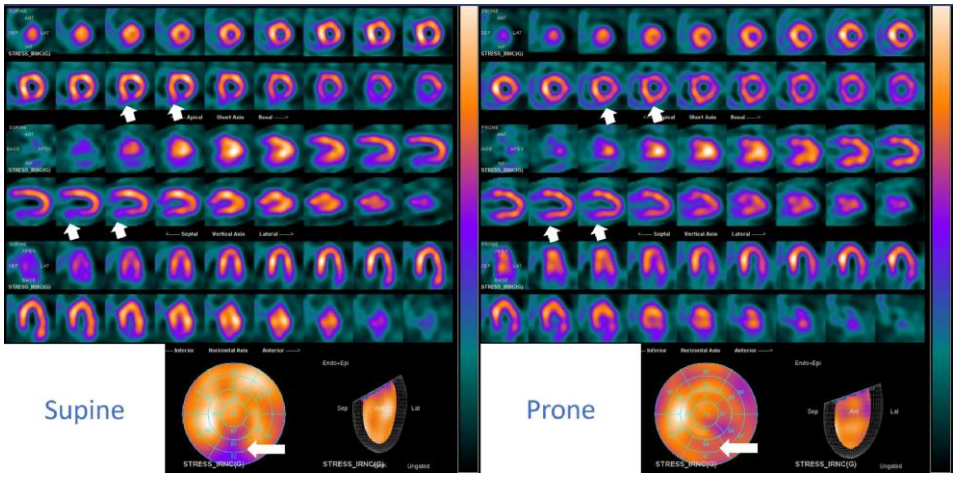

Figure 22 Supine (left) and Prone (right) post-effort SPECT images acquisitions, showing diaphragmatic attenuation (small white arrows) in sections of the LV (basal) short axis and in the VLA, also observable in the polar map (long arrows).

provides prognostic value beyond the assessment of ischaemia, as it demonstrates the presence of non-obstructive CAD.[44,45] For these reasons, the current ESC guidelines on chronic coronary syndromes recommend coronary calcium scoring with perfusion exams when CT imaging is available.[22]

Generating a clinically meaningful report

The four pillars of a clinically meaningful report include an assessment of image quality, interpretation of perfusion and gated images, evaluation of extracardiac findings, and finally, a clinical impression with risk stratification (*Figure 31*). An assessment of image quality should comment on the specific artefacts that limited interpretation of the exam, as well as the overall image quality. By including an assessment of image quality, readers are providing an impression of their diagnostic confidence.

The results of perfusion imaging should be reported in the framework of the typical vascular distribution, with specific mention of the size and severity of defects. The presence or the absence of transient ischaemic dilation or drop in LVEF should also be reported as they can be markers of high-risk.[46–49] The results of and the quality of gated imaging should also be reported.

A complete, clinical impression also requires integration of several non-MPI results. Reporting of symptoms during the exam is a key part of all stress testing, particularly in exercise protocols where clinicians can more clearly link symptoms to exertion. Functional capacity has important prognostic implications in the presence of both normal

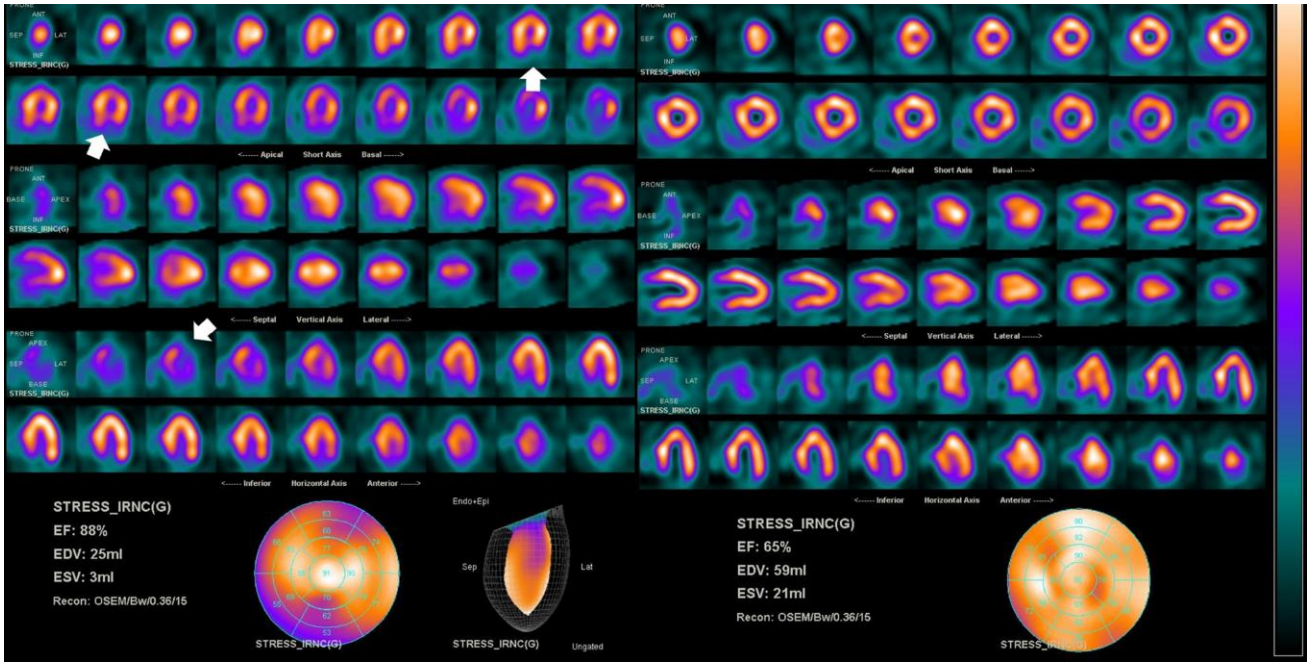

Figure 23 In this CZT acquisition, motion artefact is present on the left, showing a misleading inferior defect (arrows). The images were reacquired with the patient moving from a supine to prone position. This change in position can shift the diaphragm away from the heart and eliminate diaphragmatic attenuation. In this patient, prone imaging was more comfortable, leading to less motion during the acquisition. The motion artefact is no longer present on the right images. Note the increase in EF and the marked decrease in LV volumes that the artefact falsely presents.

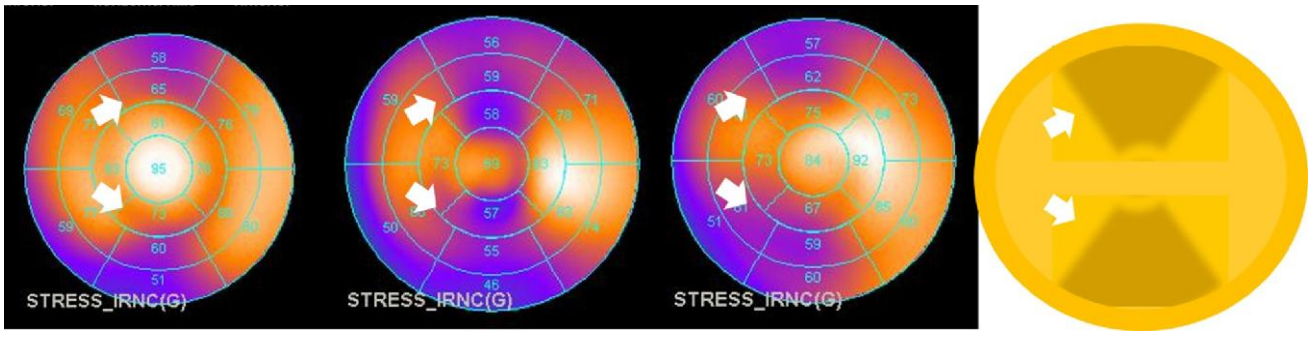

Figure 24 Three different cases of motion artefact, where a pattern often seen as a 'double inverted V' (arrows) is observed. On the right, the fourth graph corresponds to the schematic representation of the phenomenon.

and abnormal MPI and may help guide additional testing in appropriate patients.[50] Similarly, the presence of significant ECG changes can help clinicians assess post-test probability of significant CAD.[51,52] Lastly, in patients for whom CT attenuation correction was performed, a comment on the degree of coronary calcification can help guide appropriate medical therapy, even in the absence of obstructive CAD.[53]

A clinically meaningful report should therefore integrate both MPI and non-MPI results to provide a personalized and accessible report for clinicians to incorporate in their patient care.

Conclusion

MPI using nuclear molecular imaging techniques are an essential component of the practice of cardiology in the modern era. SPECT MPI can both stratify risk, as well as diagnose obstructive CAD and myocardial ischaemia. This document provides a comprehensive overview of patient preparation, the technical aspects of tracer usage, the basics of image acquisition and display, as well as potential pitfalls and artefacts that are encountered in daily practice and strategies to mitigate them.

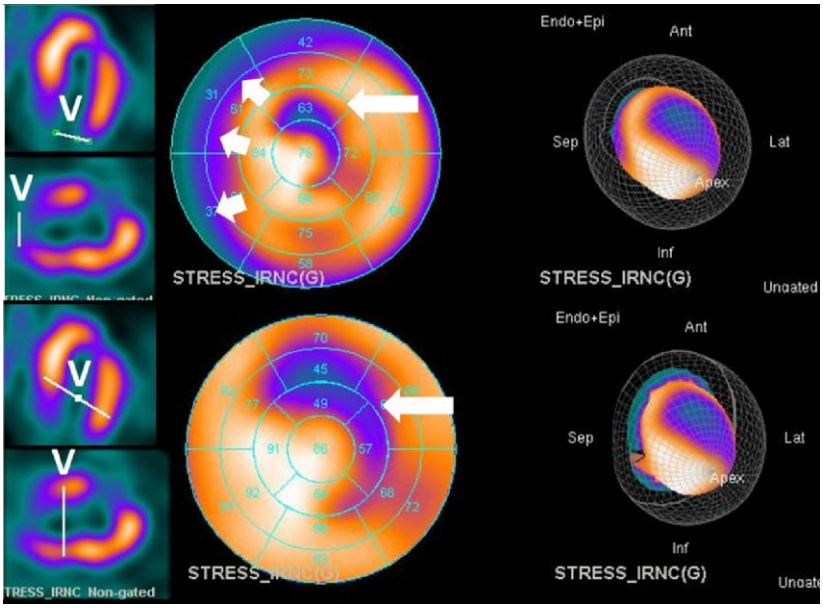

Figure 25 Left ventricle polar map views (middle) and its correspondent tomographic non-gated slices (left) and 3D rendering (right) with end diastole and perfusion layers. This shows how the poor positioning of the valve plane line marked as V (left ventricular base), has an influence on the size of the defect with the consequent under (~7% of LV in upper PM) or overestimation (~12% of LV in lower PM) of an area of hypoperfusion. In this case, there was a true defect in the territory of the diagonal artery (long arrows), but artefact in the base (short arrows).

Table 4 Common radiation dose to patients by different SPECT stress protocols and cameras[31–35]

Study protocol	Radiotracer	Typically administrated activity (mCi / *MBq*)	Estimated radiation dose (mSv)
γ-camera			
Stress only (full dose)	^{99m}Tc-sestamibi	30 / *1110*	10
1-Day Rest + Stress (half dose)	^{99m}Tc-sestamibi	5 + 15 / *185 + 555*	6.4
	^{99m}Tc-tetrofosmin	5 + 15 / *185 + 555*	5.6
2-Day Stress, Rest (half dose)	^{99m}Tc-sestamibi	5 + 5 / *185 + 185*	3.2
	^{99m}Tc-tetrofosmin	5 + 5 / *185 + 185*	2.8
1-Day Rest + Stress (full dose)	^{99m}Tc-sestamibi	10 + 30 / *370 + 1110*	13
	^{99m}Tc-tetrofosmin	10 + 30 / *370 + 1110*	11
2-Day Rest + Stress (full dose)	^{99m}Tc-sestamibi	25 + 25 / *925 + 925*	15.6
	^{99m}Tc-tetrofosmin	25 + 25 / *925 + 925*	13.5
CZT-camera			
Stress only (ultra-low dose)	^{99m}Tc-sestamibi	3.5 / *130*	1.2
Stress only (low dose)	^{99m}Tc-sestamibi	8 / *296*	2.7
2-Day Stress, Rest	^{99m}Tc-sestamibi	8 + 8/ *296 + 296*	5.4
1-Day Rest + Stress	^{99m}Tc- tetrofosmin	6 + 20 / *222 + 740*	6
1-Day Rest + Stress	^{99m}Tc-sestamibi	5 + 15 / *185 + 555*	5.8

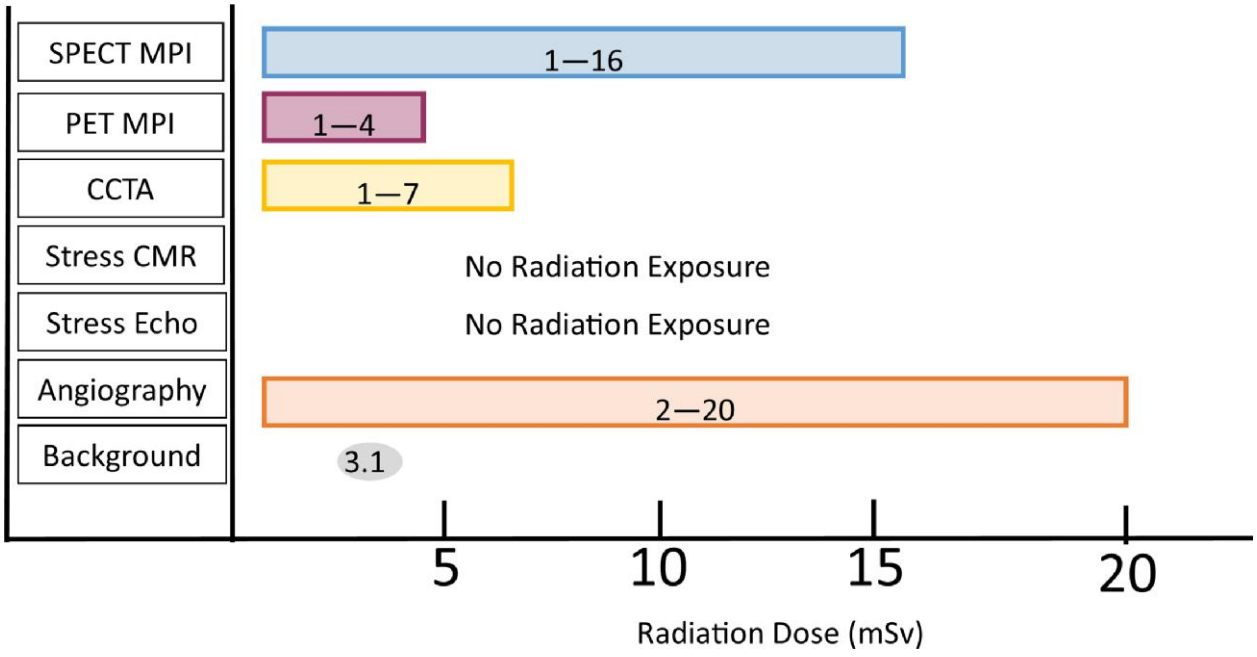

Figure 26 A comparison of radiation exposure for various cardiac imaging modalities. The typical background radiation exposure is 3.1 mSv. Of note, there is a wide variation in radiation exposure among the modalities based on technique, equipment, protocols, and patient factors. The radiation dose of PET MPI will be larger if viability imaging is performed. SPECT MPI, single-photon emission computed tomography myocardial perfusion imaging; PET MPI, positron emission computed tomography myocardial perfusion imaging; CCTA, coronary computed tomography angiography; CMR, cardiac magnetic resonance; Echo, echocardiography.[16]

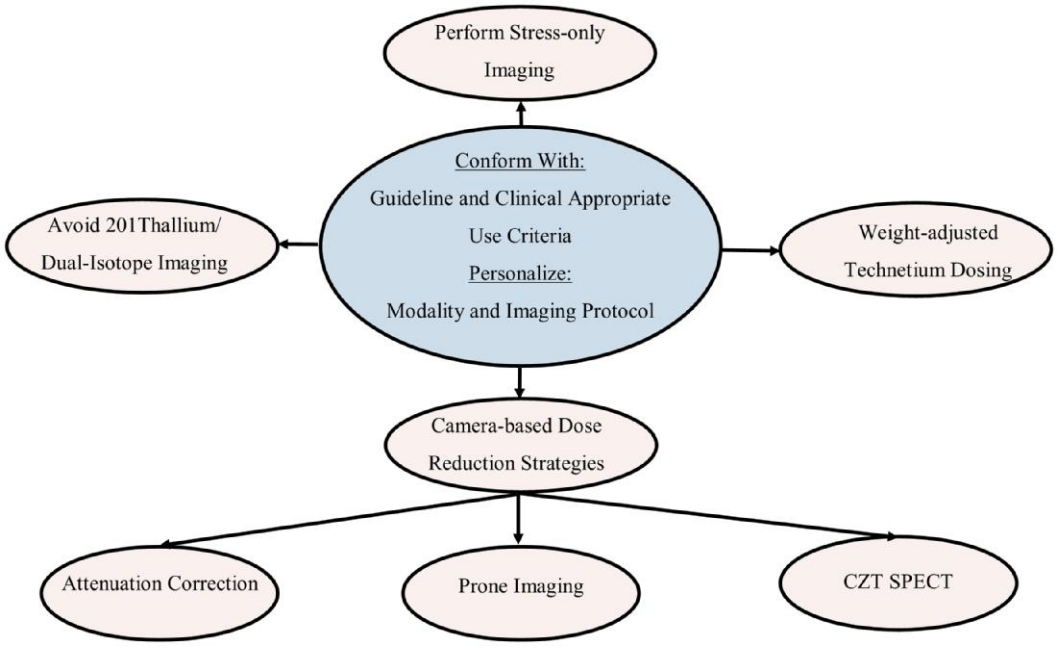

Figure 27 Radiation reduction strategies and best practices for SPECT MPI.[31,34]

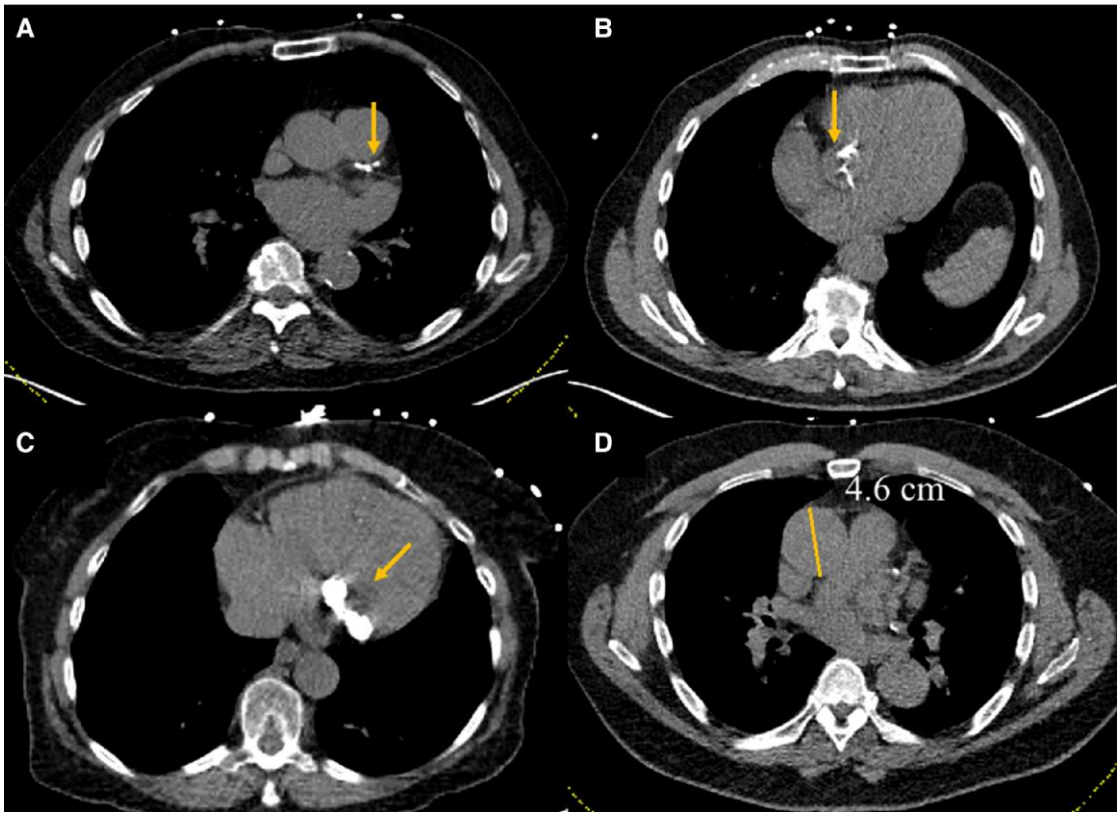

Figure 28 Incidental cardiovascular findings in CT performed for attenuation correction. (*A*) Distinct coronary calcifications should be noted. (*B*) Aortic valve and (*C*) mitral annular calcifications should prompt further evaluation with echocardiography. (*D*) Ascending aortic enlargement should also lead to dedicated evaluations.

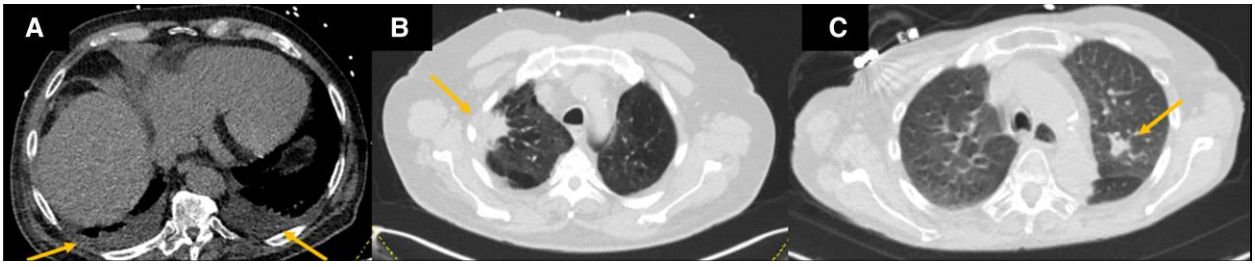

Figure 29 Incidental lung findings on CT performed for attenuation correction. Small bilateral pleural effusions are noted (*A*). A lung mass in the right upper lobe in a background of emphysema is evident (*B*). A lung nodule is observed in the left upper lobe (*C*).

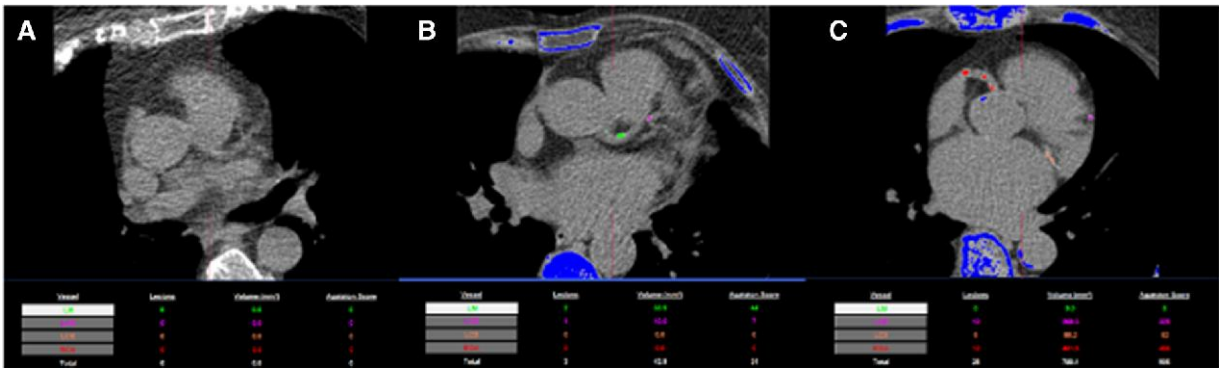

Figure 30 Dedicated coronary artery calcium scanning as part of a rest–stress myocardial perfusion study. No (*A*), mild (*B*), and severe (*C*) coronary calcifications are noted.

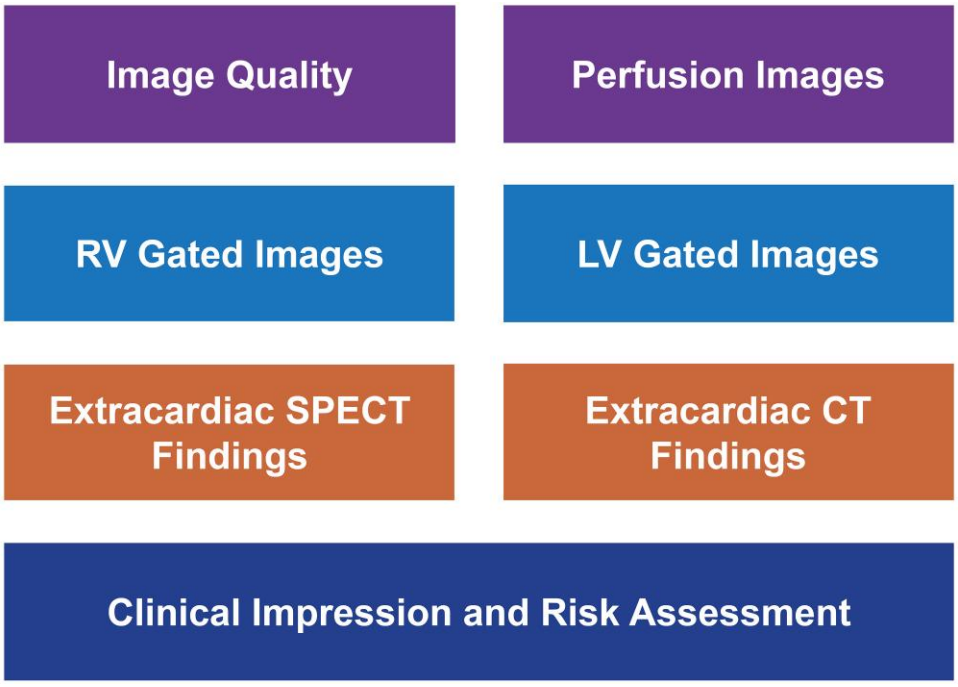

Figure 31 Components of a clinically meaningful report.

Acknowledgements

This document was reviewed by members of the 2022–2024 EACVI Scientific Documents Committee: Philippe Bertrand, Yohann Bohbot, Erwan Donal, Marc Dweck, Niall Keenan and Valtteri Uusitalo.

Conflict of interest: A.A.G. is supported by research funding grants from the Promedica Foundation and Max and Sophielène Iten-Kohaut Foundation. F.H. has received consultant and speaker fees from Bracco Imaging, Cisbio International, and GE healthcare, and he is a shareholder in Naogen Pharma. A.S. has received fees for lectures or consultancy from Abbot, Astra Zeneca, BMS, Janssen, Novo Nordisk, and Pfizer. R.S. reports unrestricted research grants of Siemens Healthineers and Pfizer. W.J. is on the board of directors of the executive council of the American Society of Nuclear Cardiology. The remainder authors have no relevant disclosures.

Funding

There was no funding for this article.

Data availability

There is no new data associated with this article.

Lead author biography

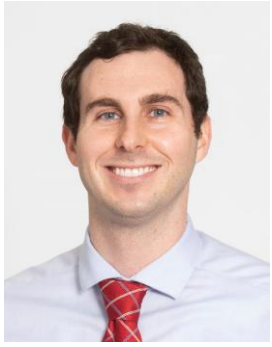

Dr. Bryan Abadie is cardiologist at the Cleveland Clinic with an interest in multimodality imaging.

References

1. Myers J, Froelicher VF. Optimizing the exercise test for pharmacological investigations. *Circulation* 1990;**82**:1839–46.
2. Mark DB, Shaw L, Harrell FE Jr, Hlatky MA, Lee KL, Bengtson JR *et al.* Prognostic value of a treadmill exercise score in outpatients with suspected coronary artery disease. *N Engl J Med* 1991;**325**:849–53.
3. Lauer MS, Francis GS, Okin PM, Pashkow FJ, Snader CE, Marwick TH. Impaired chronotropic response to exercise stress testing as a predictor of mortality. *JAMA* 1999;**281**:524–9.
4. Harb SC, Bhat P, Cremer PC, Wu Y, Cremer LJ, Berger S *et al.* Prognostic value of functional capacity in different exercise protocols. *J Am Heart Assoc* 2020;**9**:e015986.
5. Henzlova MJ, Duvall WL, Einstein AJ, Travin MI, Verberne HJ. ASNC imaging guidelines for SPECT nuclear cardiology procedures: stress, protocols, and tracers. *J Nucl Cardiol* 2016;**23**:606–39.
6. Dorbala S, Ananthasubramaniam K, Armstrong IS, Chareonthaitawee P, DePuey EG, Einstein AJ *et al.* Single Photon Emission Computed Tomography (SPECT) myocardial perfusion imaging guidelines: instrumentation, acquisition, processing, and interpretation. *J Nucl Cardiol* 2018;**25**:1784–846.
7. Brink HL, Dickerson JA, Stephens JA, Pickworth KK. Comparison of the safety of adenosine and regadenoson in patients undergoing outpatient cardiac stress testing. *Pharmacotherapy* 2015;**35**:1117–23.
8. Donal E, Lip GY, Galderisi M, Goette A, Shah D, Marwan M *et al.* EACVI/EHRA expert consensus document on the role of multi-modality imaging for the evaluation of patients with atrial fibrillation. *Eur Heart J Cardiovasc Imaging* 2016;**17**:355–83.
9. Burrell S, MacDonald A. Artifacts and pitfalls in myocardial perfusion imaging. *J Nucl Med Technol* 2006;**34**:193–211.
10. Meredith D, Cremer PC, Harb SC, Xu B, Mentias A, Jaber WA. Initial experience with regadenoson stress positron emission tomography in patients with left bundle branch block: low prevalence of septal defects and high accuracy for obstructive coronary artery disease. *J Nucl Cardiol* 2021;**28**:536–42.
11. Gibbons RJ, Balady GJ, Beasley JW, Bricker JT, Duvernoy WF, Froelicher VF *et al.* ACC/AHA guidelines for exercise testing: executive summary. A report of the American College of Cardiology/American Heart Association Task Force on Practice Guidelines (Committee on Exercise Testing). *Circulation* 1997;**96**:345–54.
12. Verberne HJ, Acampa W, Anagnostopoulos C, Ballinger J, Bengel F, De Bondt P *et al.* EANM procedural guidelines for radionuclide myocardial perfusion imaging with SPECT and SPECT/CT: 2015 revision. *Eur J Nucl Med Mol Imaging* 2015;**42**:1929–40.
13. Koepfli P, Wyss CA, Namdar M, Klainguti M, von Schulthess GK, Lüscher TF *et al.* Beta-adrenergic blockade and myocardial perfusion in coronary artery disease: differential effects in stenotic versus remote myocardial segments. *J Nucl Med* 2004;**45**:1626–31.
14. Reyes E, Stirrup J, Roughton M, D'Souza S, Underwood SR, Anagnostopoulos C. Attenuation of adenosine-induced myocardial perfusion heterogeneity by atenolol and other cardioselective beta-adrenoceptor blockers: a crossover myocardial perfusion imaging study. *J Nucl Med* 2010;**51**:1036–43.
15. Hajjiri MM, Leavitt MB, Zheng H, Spooner AE, Fischman AJ, Gewirtz H. Comparison of positron emission tomography measurement of adenosine-stimulated absolute myocardial blood flow versus relative myocardial tracer content for physiological assessment of coronary artery stenosis severity and location. *JACC Cardiovasc Imaging* 2009;**2**:751–8.
16. Hirshfeld JW Jr, Ferrari VA, Bengel FM, Bergersen L, Chambers CE, Einstein AJ *et al.* 2018 ACC/HRS/NASCI/SCAI/SCCT expert consensus document on optimal use of ionizing radiation in cardiovascular imaging: best practices for safety and effectiveness: a report of the American College of Cardiology Task Force on Expert Consensus Decision Pathways. *J Am Coll Cardiol* 2018;**71**:e283–351.
17. Hyafil F, Gimelli A, Slart RHJA, Georgoulias P, Rischpler C, Lubberink M *et al.* EANM procedural guidelines for myocardial perfusion scintigraphy using cardiac-centered gamma cameras. *Eur J Hybrid Imaging* 2019;**3**:11.
18. Bocher M, Blevis IM, Tsukerman L, Shrem Y, Kovalski G, Volokh L. A fast cardiac gamma camera with dynamic SPECT capabilities: design, system validation and future potential. *Eur J Nucl Med Mol Imaging* 2010;**37**:1887–902.
19. Esteves FP, Raggi P, Folks RD, Keidar Z, Askew JW, Rispler S *et al.* Novel solid-state-detector dedicated cardiac camera for fast myocardial perfusion imaging: multicenter comparison with standard dual detector cameras. *J Nucl Cardiol* 2009;**16**:927–34.
20. Buechel RR, Kaufmann PA, Gaemperli O. 3-Single-photon emission computed tomography. In: Nieman K, Gaemperli O, Lancellotti P, Plein S, eds. *Advanced Cardiac Imaging*. Cambridge: Elsevier; 2015. p.47–69.
21. Marcassa C, Zoccarato O. Advances in image reconstruction software in nuclear cardiology: is all that glitters gold? *J Nucl Cardiol* 2017;**24**:142–4.
22. Vrints C, Andreotti F, Koskinas KC, Rossello X, Adamo M, Ainslie J *et al.* 2024 ESC guidelines for the management of chronic coronary syndromes: developed by the task force for the management of chronic coronary syndromes of the European Society of Cardiology (ESC) endorsed by the European Association for Cardio-Thoracic Surgery (EACTS). *Eur Heart J* 2024;**45**:3415–537.
23. Wells RG, Trottier M, Premaratne M, Vanderwerf K, Ruddy TD. Single CT for attenuation correction of rest/stress cardiac SPECT perfusion imaging. *J Nucl Cardiol* 2018;**25**:616–24.
24. Johnson RD, Bath NK, Rinker J, Fong S, St. James S, Pampaloni MH *et al.* Introduction to the D-SPECT for technologists: workflow using a dedicated digital cardiac camera. *J Nucl Med Technol* 2020;**48**:297–303.
25. Cerqueira MD, Weissman NJ, Dilsizian V, Jacobs AK, Kaul S, Laskey WK *et al.* Standardized myocardial segmentation and nomenclature for tomographic imaging of the heart. A statement for healthcare professionals from the Cardiac Imaging Committee of the Council on Clinical Cardiology of the American Heart Association. *Circulation* 2002;**105**:539–42.
26. Kumar A, Patel DR, Harb SC, Greenberg NL, Bhargava A, Menon V *et al.* Implementation of a myocardial perfusion imaging risk algorithm to inform appropriate downstream invasive testing and treatment. *Circ Cardiovasc Imaging* 2021;**14**:e011984.
27. Kakhki VRD, Sadeghi R, Zakavi SR. Assessment of transient left ventricular dilation ratio via 2-day dipyridamole Tc-99m sestamibi nongated myocardial perfusion imaging. *J Nucl Cardiol* 2007;**14**:529–36.
28. Leslie WD, Tully SA, Yogendran MS, Ward LM, Nour KA, Metge CJ. Prognostic value of lung sestamibi uptake in myocardial perfusion imaging of patients with known or suspected coronary artery disease. *J Am Coll Cardiol* 2005;**45**:1676–82.
29. Ferro A, Petretta M, Acampa W, Fiumara G, Daniele S, Petretta MP *et al.* Post-stress left ventricular ejection fraction drop in patients with diabetes: a gated myocardial perfusion imaging study. *BMC Cardiovasc Disord* 2013;**13**:99.
30. Ioannidis JPA, Trikalinos TA, Danias PG. Electrocardiogram-gated single-photonemission computed tomography versus cardiacmagnetic resonance imaging for the assessmentof left ventricular volumes and ejection fraction: a meta-analysis. *J Am Coll Cardiol* 2002;**39**:2059–68.
31. Dorbala S, Blankstein R, Skali H, Park MA, Fantony J, Mauceri C *et al.* Approaches to reducing radiation dose from radionuclide myocardial perfusion imaging. *J Nucl Med* 2015;**56**:592–9.
32. Desiderio MC, Lundbye JB, Baker WL, Farrell MB, Jerome SD, Heller GV. Current status of patient radiation exposure of cardiac positron emission tomography and single-photon emission computed tomographic myocardial perfusion imaging. *Circ Cardiovasc Imaging* 2018;**11**:e007565.
33. Case JA, deKemp RA, Slomka PJ, Smith MF, Heller GV, Cerqueira MD. Status of cardiovascular PET radiation exposure and strategies for reduction: an information statement from the cardiovascular PET task force. *J Nucl Cardiol* 2017;**24**:1427–39.
34. Gimelli A, Achenbach S, Buechel RR, Edvardsen T, Francone M, Gaemperli O *et al.* Strategies for radiation dose reduction in nuclear cardiology and cardiac computed tomography imaging: a report from the European Association of Cardiovascular Imaging (EACVI), the Cardiovascular Committee of European Association of Nuclear Medicine (EANM), and the European Society of Cardiovascular Radiology (ESCR). *Eur Heart J* 2018;**39**:286–96.
35. Maddahi J, Agostini D, Bateman TM, Bax JJ, Beanlands RSB, Berman DS *et al.* Flurpiridaz F-18 PET myocardial perfusion imaging in patients with suspected coronary artery disease. *J Am Coll Cardiol* 2023;**82**:1598–610.
36. Lim P, Agarwal V, Patel KK. How to assess nonresponsiveness to vasodilator stress. *J Nucl Cardiol* 2024;**36**:101850.

37. Cerqueira MD, Allman KC, Ficaro EP, Hansen CL, Nichols KJ, Thompson RC *et al.* Recommendations for reducing radiation exposure in myocardial perfusion imaging. *J Nucl Cardiol* 2010;**17**:709–18.
38. Einstein AJ. High radiation doses from SPECT myocardial perfusion imaging in the United States. *Circ Cardiovasc Imaging* 2018;**11**:e008383.
39. Dorbala S, Di Carli MF, Delbeke D, Abbara S, DePuey EG, Dilsizian V *et al.* SNMMI/ASNC/SCCT guideline for cardiac SPECT/CT and PET/CT 1.0. *J Nucl Med* 2013;**54**:1485–507.
40. Dickson JC, Armstrong IS, Gabiña PM, Denis-Bacelar AM, Krizsan AK, Gear JM *et al.* EANM practice guideline for quantitative SPECT-CT. *Eur J Nucl Med Mol Imaging* 2023;**50**:980–95.
41. Genovesi D, Giorgetti A, Gimelli A, Gimelli A, Kusch A, D'Aragona Tagliavia I *et al.* Impact of attenuation correction and gated acquisition in SPECT myocardial perfusion imaging: results of the multicentre SPAG (SPECT attenuation correction vs gated) study. *Eur J Nucl Med Mol Imaging* 2011;**38**:1890–8.
42. Alessio AM, Kohlmyer S, Branch K, Chen G, Caldwell J, Kinahan P *et al.* Cine CT for attenuation correction in cardiac PET/CT. *J Nucl Med* 2007;**48**:794–801.
43. Kay F, Canan A, Abbara S. Common incidental findings on cardiac CT: a systematic review. *Curr Cardiovasc Imaging Rep* 2019;**12**:1–12.
44. Mouden M, Timmer JR, Reiffers S, Oostdijk AHJ, Knollema S, Ottervanger JP *et al.* Coronary artery calcium scoring to exclude flow-limiting coronary artery disease in symptomatic stable patients at low or intermediate risk. *Radiology* 2013;**269**:77–83.
45. Engbers EM, Timmer JR, Ottervanger JP, Mouden M, Knollema S, Jager PL. Prognostic value of coronary artery calcium scoring in addition to single-photon emission computed tomographic myocardial perfusion imaging in symptomatic patients. *Circ Cardiovasc Imaging* 2016;**9**:e003966.
46. Abidov A, Bax JJ, Hayes SW, Hachamovitch R, Cohen I, Gerlach J *et al.* Transient ischemic dilation ratio of the left ventricle is a significant predictor of future cardiac events in patients with otherwise normal myocardial perfusion SPECT. *J Am Coll Cardiol* 2003;**42**:1818–25.
47. Abidov A, Germano G, Berman DS. Transient ischemic dilation ratio: a universal high-risk diagnostic marker in myocardial perfusion imaging. *J Nucl Cardiol* 2007;**14**:497–500.
48. Dona M, Massi L, Settimo L, Bartolini M, Giannì G, Pupi A *et al.* Prognostic implications of post-stress ejection fraction decrease detected by gated SPECT in the absence of stress-induced perfusion abnormalities. *Eur J Nucl Med Mol Imaging* 2011;**38**:485–90.
49. Sharir T, Germano G, Kavanagh PB, Lai S, Cohen I, Lewin HC *et al.* Incremental prognostic value of post-stress left ventricular ejection fraction and volume by gated myocardial perfusion single photon emission computed tomography. *Circulation* 1999;**100**:1035–42.
50. McNeer JF, Margolis JR, Lee KL, Kisslo JA, Peter RH, Kong Y *et al.* The role of the exercise test in the evaluation of patients for ischemic heart disease. *Circulation* 1978;**57**:64–70.
51. Marshall ES, Raichlen JS, Kim SM, Intenzo CM, Sawyer DT, Brody EA *et al.* Prognostic significance of ST-segment depression during adenosine perfusion imaging. *Am Heart J* 1995;**130**:58–66.
52. Goldschlager N, Selzer A, Cohn K. Treadmill stress tests as indicators of presence and severity of coronary artery disease. *Ann Intern Med* 1976;**85**:277–86.
53. Detrano R, Guerci AD, Carr JJ, Bild DE, Burke G, Folsom AR *et al.* Coronary calcium as a predictor of coronary events in four racial or ethnic groups. *N Engl J Med* 2008;**358**:1336–45.